Observations of the phase-locked 2 day wave over the Australian sector using medium-frequency radar and airglow data

J. H. Hecht,[1] R. L. Walterscheid,[1] L. J. Gelinas,[1] R. A. Vincent,[2] I. M. Reid,[2] and J. M. Woithe[2]

Received 28 December 2009; revised 31 March 2010; accepted 7 April 2010; published 25 August 2010.

[1] The quasi 2 day wave, with a nominal mean period just above 50 h, is a significant feature of the 80–100 km altitude region in both hemispheres. It becomes particularly prominent in the Southern Hemisphere summer at midlatitudes where, a short time after summer solstice, its amplitude rapidly increases and its mean period is found to be approximately 48 h, producing an oscillation phase locked in local time. This lasts for a few weeks. Presented here are observations of the meridional winds and airglow over two sites in Australia, for 4 years during the austral summers of 2003–2006. We show that during those times when the large-amplitude phase-locked 2 day wave (PL-TDW) is present the diurnal tide greatly decreases. This is consistent with the Walterscheid and Vincent (1996) model in which the PL-TDW derives its energy from a parametric excitation by the diurnal tide. These data also show that the diurnal tide is more suppressed and the PL-TDW amplitude is larger in odd-numbered years, suggesting a biannual effect. The airglow data indicated that, for the PL-TDW, the winds and temperature are nearly out of phase. When the PL-TDW is present airglow amplitudes can become quite large, a result dependent on the local time of the PL-TDW maximum. The airglow intensity response was, in general, much larger than what would be expected from the airglow temperature response, suggesting that the PL-TDW is causing a significant composition change possibly due to minor constituent transport.

Citation: Hecht, J. H., R. L. Walterscheid, L. J. Gelinas, R. A. Vincent, I. M. Reid, and J. M. Woithe (2010), Observations of the phase-locked 2 day wave over the Australian sector using medium-frequency radar and airglow data, *J. Geophys. Res.*, *115*, D16115, doi:10.1029/2009JD013772.

1. Introduction

[2] The quasi 2 day wave (QTDW) is a significant planetary-scale feature of the 80–100 km region that is seen in both hemispheres most prominently after summer solstice. The QTDW was apparently first reported on in a Ph.D. thesis at the University of Adelaide on meteor wind observations [*Doyle*, 1968]. Subsequent to that study additional ground-based wind observations were reported that described this phenomenon more fully in the Northern and Southern hemispheres [e.g., *Muller and Nelson*, 1978; *Craig and Elford*, 1981] and in the equatorial regions [e.g., *Harris and Vincent*, 1993].

[3] In the Northern Hemisphere midlatitude region the QTDW may be present much of the year at a low amplitude of a few m/s. However, it becomes strongest after summer solstice where amplitudes reach on the order of 20 m/s. The period of this wave is somewhat above 50 h, hence the designation as the QTDW, with mean periods measured close to 51 h by *Muller and Nelson* [1978] and near 53 h by *Tsuda et al.* [1988]. The amplification of the QTDW during the summer is rather gradual, and the QTDW often persists near maximum amplitude for 1 or 2 months.

[4] In the Southern Hemisphere midlatitudes however, its character is different. Just after summer solstice, during January/February, the wave amplitude rapidly increases reaching 50 m/s or more, over twice that seen in the Northern Hemisphere. This amplification is rapid and the duration of the event is more pulse like than in the Northern Hemisphere. Near Adelaide, Australia, where data has been acquired for over 40 years, the wave mean period is close to 48 h and thus, is phase locked, with the wave maximum occurring at nearly the same local time from cycle to cycle. *Harris* [1994] reported that from the 1960s through 1992 this local time was most often in the post noon sector with a mean around 1400 LT. Thus, this wave is more aptly referred to as a phase-locked 2 day wave (PL-TDW).

[5] This phase locking is also seen in the equatorial regions, and extending across the equator into the low-latitude Northern Hemisphere. However, close to the equator a QTDW with a period near 50 h is present at a fairly large amplitude much of the year. Because of this the appearance after

[1]Space Sciences Department, The Aerospace Corporation, Los Angeles, California, USA.
[2]Department of Physics and Mathematical Physics, University of Adelaide, Adelaide, South Australia, Australia.

0148-0227/10/2009JD013772

Southern Hemisphere summer solstice of the amplified PL-TDW at a period near 48 h is not as dramatic as at Adelaide [*Harris and Vincent*, 1993].

[6] There are several interesting aspects of the PL-TDW. Its strength is anticorrelated with the strength of the diurnal tide both near the equator [*Harris and Vincent*, 1993] and at Adelaide [*Harris*, 1994]. *Harris and Vincent* [1993] also noted the presence of a 16 h wave, reported on earlier by *Manson and Meek* [1990]. This 16 h wave might be due to a nonlinear interaction of a 2 day wave and the diurnal or semidiurnal tide. This interaction would, in addition, produce a 9.6 h wave which was indeed seen in the equatorial data [e.g., *Pancheva*, 2006; *Walterscheid and Vincent*, 1996].

[7] These observations inspired a number of investigations that attempted to model this phenomenon. There are basically two explanations for the QTDW. The earliest by *Salby* [1981] suggested that the QTDW was a Rossby normal mode. The other by *Plumb* [1983] suggested that it was due to a baroclinic instability of the extratropical stratospheric westward winds. We suggest that whatever mechanism explains the QTWD, the PL-TDW is the result of a subharmonic instability involving a normal mode with a period very close to twice the period of the diurnal tide. The theoretical problem for the summertime Southern Hemisphere PL-TDW is to account for its sudden commencement, stability, and phase locking. Neither a simple normal mode response without an excitation mechanism nor a baroclinic instability offers a plausible explanation for the observed phase locking and sudden amplification.

[8] *Walterscheid and Vincent* [1996] addressed this by proposing that the PL-TDW is a near resonant wave forced parametrically by the diurnal tide. The sudden onset is the result of the tuning of the normal mode QTDW to a period close to a subharmonic of the diurnal tide [*Hagan et al.*, 1993]. The tuning of the resonant frequency to a subharmonic frequency of the diurnal tide would produce a dramatic decrease in the diurnal tidal amplitude since the diurnal tide first pumps the PL-TDW to bring it to large amplitude and then sustains it after the PL-TDW reaches large amplitude. Once the PL-TDW has attained its limiting amplitude it can be sustained by a smaller amplitude diurnal tide. The tuning required to produce the PL-TDW may explain why it does not occur in the Northern Hemisphere summer [*Hagan et al.*, 1993]. The *Walterscheid and Vincent* [1996] study also showed that the observed 16 h component could be produced by interactions involving the diurnal tide and 2 day wave. (Hereafter we will use TDW to broadly represent a 2 day wave whether a QTDW or a PL-TDW.)

[9] Following this work, *Palo et al.* [1998] investigated the presence of a TDW for mid-January conditions using the TIME-GCM. They found a strong TDW which peaked around 90 km altitude near 30°S latitude that appeared to be the result of forcing by the diurnal tide and was thus the PL-TDW. In the numerical experiment the PL-TDW was seen as far south as 80°S, and as far north as 30°N. Interestingly, they found a key mediatory of the interactions scheme suggested by *Walterscheid and Vincent* [1996], namely the westward wave number six (W6) diurnal tide. This tide had not been previously seen in TIME-GCM runs. *Palo et al.* [1998] also noted that the diurnal tide was reduced by about 20% compared to periods when the PL-TDW was not present. Although there have been many studies since then, there has been little further investigation into the nature of the PL-TDW. In this study we address the following questions:

[10] First, how is the occurrence of the PL-TDW related to changes in (1) the diurnal and (2) the semidiurnal tide?

[11] 1. The earlier observational studies cited above used Fourier techniques that do not capture fully the evolution of a transient event. Two recent studies, however, analyzed data with wavelet techniques designed to capture such features. Although neither analysis was for a midlatitude Southern Hemisphere site, where the PL-TDW is strong and the QTDW is quite weak, they do provide some information on the relation between the PL-TDW and the tides. *Lima et al.* [2004] analyzed data taken during the austral summer at 22°S latitude and showed an apparent anticorrelation between the amplitude of a TDW and the amplitude of the diurnal tide. However, they do not discuss these data in the context of the PL-TDW model of *Walterscheid and Vincent* [1996]. *Pancheva* [2006] also showed such an anticorrelation from wind data taken at Ascension Island (9°S) during early 2003. This study notes that the anticorrelation occurred when the TDW period was close to 48 h, and thus, as defined above, is a PL-TDW. This report noted that the anticorrelation was consistent with the *Palo et al.* [1998] and *Walterscheid and Vincent* [1996] studies.

[12] 2. When the QTDW was present a 2 day wavelike modulation of the diurnal and semidiurnal tides also occurred in the *Pancheva* [2006] data. Most of that study was devoted to analyzing this interaction. However, these data also showed such modulations occurring during the PL-TDW period, the significance of which was not discussed.

[13] Second, what is the variation of temperature during PL-TDW events? While most of the observations of the PL-TDW were of wind amplitudes there have been some satellite observations of the temperature field [*Rodgers and Prata*, 1981; *Fritts et al.*, 1999]. The latter show UARS data from the HRDI instrument. Their results also suggested an uncertain relationship between the time of the maximum wind and temperature response with the maximum temperature response sometimes being simultaneous and sometimes preceding the wind maximum. However, because the UARS satellite essentially sampled one local time, the exact period of the TDW was uncertain.

[14] Third, what is the airglow response during a PL-TDW event? A PL-TDW event can affect the airglow in several ways. The wave-induced vertical motions, acoustic compressibility, and associated temperature changes should affect the composition and chemistry which would then result in airglow intensity and temperature variations [e.g., *Hecht*, 2004; *Hickey et al.*, 1993]. (Note that idealized normal modes are Lamb waves for which the vertical velocity is nil and for such waves temperature and transport related changes would be caused by the acoustic effects of compressibility rather than the static effects.) If a wave is undergoing a transient build up (or decay) related to an instability this can induce transport that can affect airglow intensity. Finally, as *Plumb et al.* [1987] and *Harris* [1994] pointed out a 2 day wave with a wind amplitude of 55 m/s would transport a parcel of air on the order of 3000 km in a day. Such transport across horizontal gradients could certainly affect atmospheric composition and thus, airglow intensities.

[15] There have been only a few reports of the airglow response during TDW events. *Ward et al.* [1997] reported

Table 1. Airglow Means for Years 2003 and 2004

Site[a]	Parameter	Mean	Threshold	Percent Above Threshold
BP	OHI	1376	2000	11
BP	OHT	191	210	10
BP	O2I	440	600	19
BP	O2T	186	200	16
AS	OHI	1430	2000	12
AS	OHT	192	210	6
AS	O2I	356	600	8
AS	O2T	182	200	6

[a]Alice Springs (AS) and Buckland Park (BP).

on OI (557.7 nm) green line airglow from UARS satellite observations during mid-January 1993. They found enhanced airglow due to vertical motions without evidence of mixing due to wave breaking and instabilities. Unfortunately, the observations were from the Northern Hemisphere so that the PL-TDW was probably not observed. *Takahashi et al.* [2005] reported observations from an equatorial site of the same airglow which is the subject of this paper, the OH Meinel and O2 Atmospheric band emissions. They reported an airglow response to the QTDW that did at times produce large airglow intensities. But their results excluded the January and February periods and thus again the PL-TDW was probably not seen.

[16] This work will address aspects of these questions using three sets of data, one of which is of wind data, and the other two are of airglow data. First, we will report on meridional wind data from Buckland Park, Australia (about 30 km north of Adelaide) where data has been obtained since the 1960s. Unlike the earlier analysis of Buckland Park data, wavelet techniques will be used to investigate the first question. Next we will discuss simultaneous airglow data taken from two sites in Australia: at Buckland Park collocated with an MF wind radar, and at Alice Springs about 1500 km north of Adelaide. These data sets have been obtained since 2001 and have recently been the subject of a study on airglow climatology including temperature and intensity [*Gelinas et al.*, 2008]. The main periods reported on here are from the months of January, February, and early March during the years 2003–2006 where for the most part continuous wind and airglow data are available.

2. Experimental Instrumentation and Technique

2.1. Instrumentation

2.1.1. MF Radar at Buckland Park

[17] An MF radar is located at Buckland Park (34.9°S, 138.6°E), some 35 km north of Adelaide. Operating at 1.98 MHz it measures winds using the spaced antenna technique in the 60–98 km range by day and in the 80–98 km range by night. Measurements are made every 2 minutes at 2 km height intervals. Here we use hourly averaged meridional wind components. Further details about the system and techniques used may be found in the work by *Holdsworth and Reid* [2004]. The average variance for these hourly data at 88 km was about 200 m^2/s^2.

2.1.2. Airglow Imagers

[18] The airglow instruments at Buckland Park (BP) and at Alice Springs (AS), located at 23.8°S, 133.9°E, are modified versions of The Aerospace Corporation's charge coupled device (CCD) nightglow camera which was originally described by *Hecht et al.* [1994] and further described by *Hecht et al.* [2004b]. The imager now uses a 1536 by 1024 Kodak CCD chip. The pixels are binned 8 × 8, resulting in images that have 192 × 128 pixels. The angular field of view is now 69° by 46° giving a spatial field of view of approximately 122 × 75 km at 90 km altitude. This instrument obtains images of the OH Meinel (6,2) (hereinafter OHM) and O2 Atmospheric (0,1) band (hereinafter O2A) band emissions. A sequence of five images is obtained, each at 1 min integration, through separate narrow passband filters. Two of the filters cover two different rotational lines of OHM, two filters cover different portions of O2A, and one filter covers the background and has almost no airglow emission in its passband. The latter is used to correct the airglow images for background skylight. Thus, one can obtain images of the OHM and O2A airglow, the intensity and temperature of the OHM and O2A emissions, and atmospheric gravity wave horizontal wavelengths and ground-based phase velocities, [e.g., *Hecht et al.*, 1997, 2001]. For this work we discuss the OHM and O2A intensities and temperatures as determined using the techniques described by *Gelinas et al.* [2008]. Table 1 gives the mean values for each site. Note that these mean values are comparable to those reported on by *Gelinas et al.* [2008] with the exception of the O2A intensities. This was due to an error in the *Gelinas et al.* [2008] O2A intensity calibration used to determine the DC offset. This has been corrected here.

2.2. Data Analysis

[19] A main objective of this study is to determine the day to day variation of the TDW with respect to other wave components such as the tides at 12 and 24 h. Fourier transforms, which were used in the earlier studies of the QTDW and PL-TDW [e.g., *Harris and Vincent*, 1993], are not localized in time and thus are not well suited to measuring features that may be present for only a fraction of the analysis period. However, wavelet transforms are localized in frequency and in time and have been used in recent studies of the QTDW and PL-TDW [*Lima et al.*, 2004; *Pancheva et al.*, 2006; *Pancheva*, 2006]. Wavelet techniques are suited for measuring transient wavelike oscillations in the airglow emission region at 80 to 100 km altitude [*Hecht et al.*, 2007] such as the onset or disappearance of the PL-TDW.

[20] An excellent discussion of the practical use of wavelets in time series analysis is given by *Torrance and Compo* [1998]. The equations presented in that work have been coded in the Interactive Data Language and are available from Torrance. That software, which has been further modified by us, forms the basis for the analysis software used in this work. The Morlet wavelet discussed by *Torrance and Compo* [1998] has been selected here as the primary analysis tool. Such an analysis is performed over different scales beginning at twice the time separation of the data which is 1 h for the wind data. For the Morlet wavelet used in this work the equivalent Fourier period is 1.03 times the Morlet scale [*Torrance and Compo*, 1998]. For the plots in this paper Fourier periods are used.

[21] The Morlet wavelet was chosen because it is more localized in frequency, while still localized in time, than other wavelets available allowing a better separation of

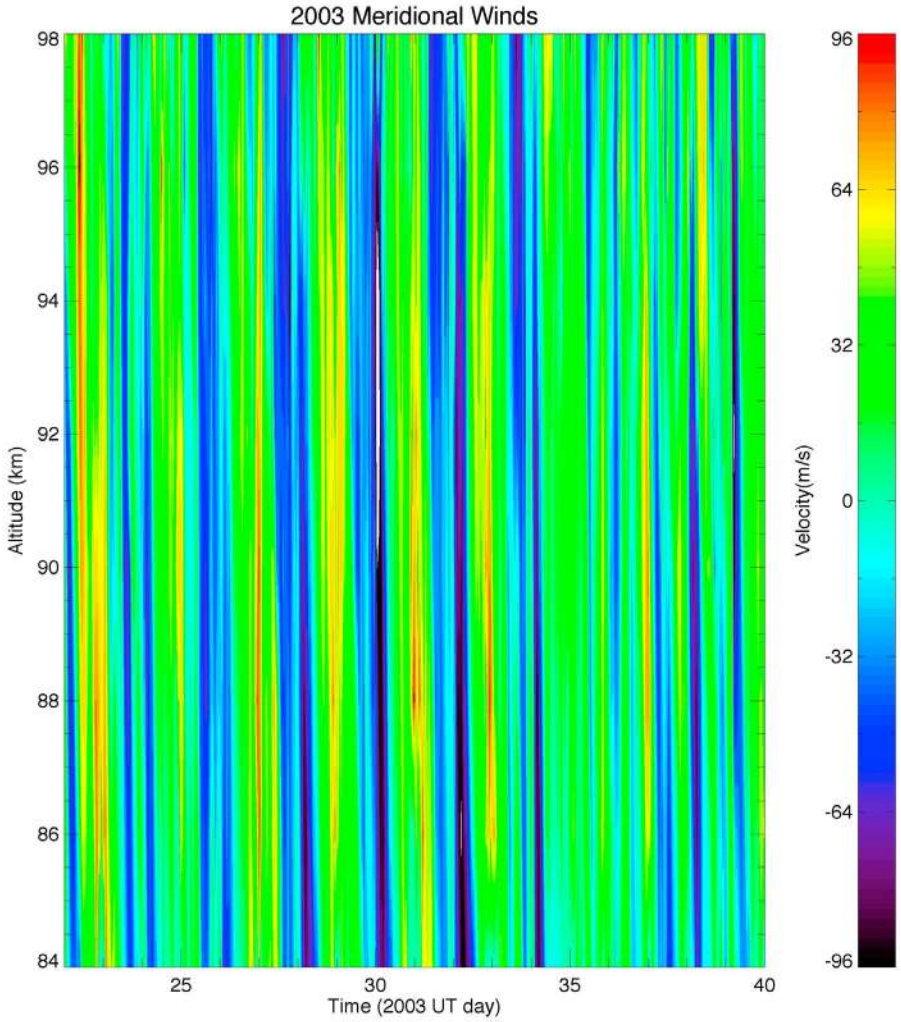

Figure 1. Image of the meridional wind velocity (in m/s) as a function of time (in 2003 UT day) and altitude (in km).

different wave period components. To check the separation we input a fixed period wave into the wavelet software and looked for power in the four band passes that are used in this paper to isolate the TDW (40–60 h), the diurnal (20–30 h) and semidiurnal (11–13 h) tides, and the 16 h (15–17 h period wave. In particular, except for the 16 h period band pass there was typically much less than 1% leakage of power between them. For the 16 h period band pass there was a leakage of about 16% into the semidiurnal tide band pass and about 2% to 3% into the diurnal tide. Both the diurnal and semidiurnal band passes leaked about 2% to 3% energy into the 16 h band pass. The reconstructed time series was generally within 1% or 2% in amplitude of the original time series.

3. Results

[22] While this work discusses results from December 2002 through March 2006, the time frame that will be emphasized is from 24 December 2002 through 2 March 2003. During that period both a strong and a weak TDW event occurred, the former being most likely a PL-TDW. Also, airglow data were available not degraded by overcast or moon up conditions. The meridional wind results will be presented first followed by the airglow results. Note that while most times are given in Universal Time (UT) we sometimes refer to Local Time (LT) as indicated. UT is used to allow comparisons with other sites away from the Australian sector. For the Australian sites LT is 9.5 h ahead of UT. UT day 1 of a year begins at 0000 (hhmm) UT on 1 January.

3.1. Data From 2003

3.1.1. Meridional Winds From Day 358 in 2002 Through Day 61 in 2003 (24 December 2002 Through 2 March 2003)

[23] Figure 1 shows a plot of the meridional wind velocities, the wind component where TDW effects are most often observed, versus altitude for days 21–40 in 2003. The color scale emphasizes large amplitude winds. TDW signatures are easily seen until about day 34 after which other wave periods dominate. The TDW maxima appear to be nearly vertical indicating that the vertical wavelength is quite large, consistent with previous observations at this site [*Harris*, 1994]. Given the large vertical wavelength of the

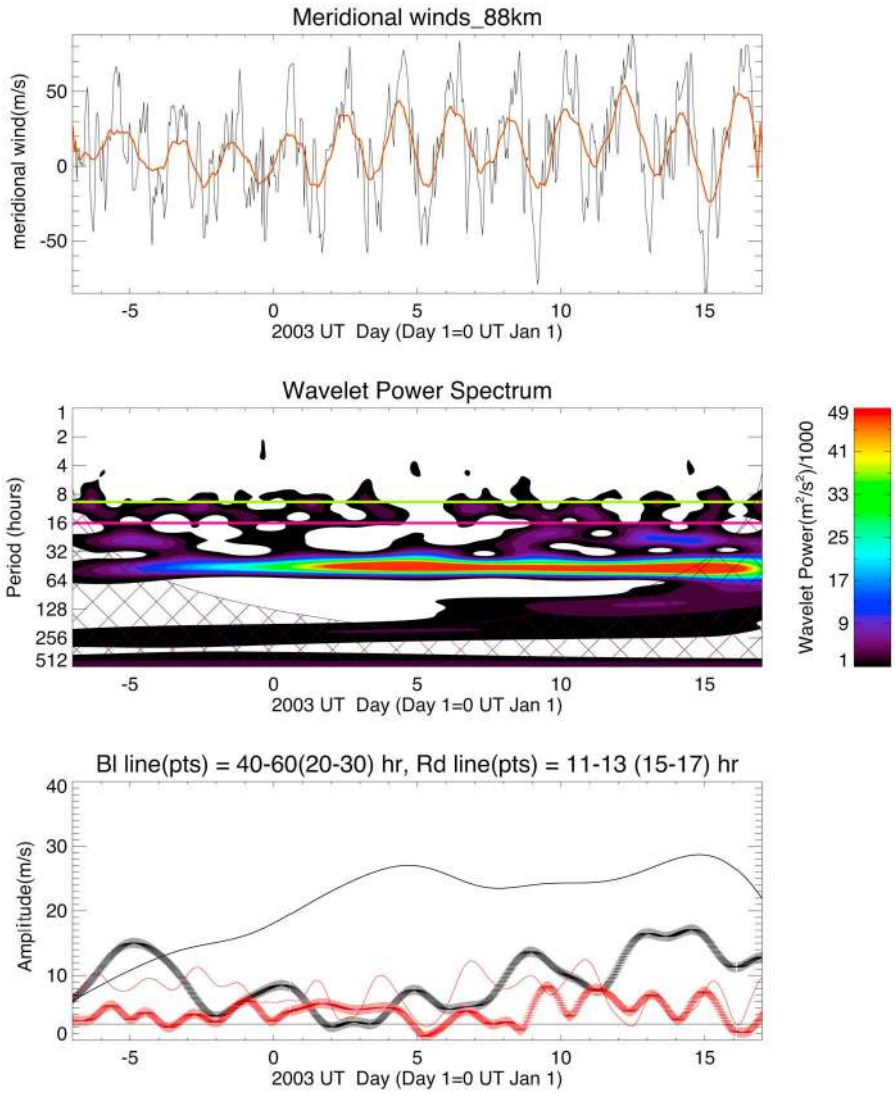

Figure 2. Results for the period from 0000 UT on 24 December 2002 to 0000 UT on 17 January 2003. (top) Black solid plot of the measured meridional wind in m/s. Red solid line shows the wind data smoothed over 24 h. (middle) The wavelet power spectrum as a function of Fourier period. The cross-hatched area is the cone of influence as defined by *Torrance and Compo* [1998]. The red (green) line shows the expected position of a 16 (9.6) h Fourier period feature. (bottom) Meridional wind amplitude (in m/s) for wavelet periods of 40–60 h (black line), 20–30 h (black pluses), 11–13 h (red line), and 15–17 h (red pluses). The horizontal line shows an estimate of the standard deviation in m/s expected in the 20–30 h band pass.

TDW the rest of the analysis will be performed at 88 km altitude where the OHM airglow volume emission rates [e.g., *Hecht et al.*, 2004a] and the TDW wind amplitudes are both large.

[24] Although the wind data are mostly continuous there was a gap from 0000 UT on day 17 through 0000 UT on day 21 and thus, Figure 2 (top) shows the meridional wind velocity from 0000 UT on day 358 in 2002 through 0000 UT on day 17 2003. Also shown is a smoothing of these data over 24 h, using a running mean, which suppresses the diurnal and semidiurnal tides. Clearly, there is a TDW component throughout this period with an amplitude approaching 30 m/s, although this magnitude may be somewhat diminished due to the smoothing process.

[25] Figure 2 (middle) shows the wavelet power spectrum as a function of Fourier period and day of year for the unsmoothed data. Only wavelet power above 1000 m^2/s^2 is shown to emphasize real signal over instrument noise. Clearly, there is a strong signal near 48 h due to a TDW. This wave dominates the spectrum. The TDW power is strongest near days 5 and 15. The cross-hatched area is the cone of influence exclusion zone where there is less confidence in the results due to edge effects [*Torrance and Compo*, 1998]. However, for these data this zone appears to be of minimal significance since the power spectrum shows a clear TDW signal at day 16 consistent with the raw data shown in the Figure 2 (top). The diurnal tide is strongest near day 360, when the TDW is absent, and is quite

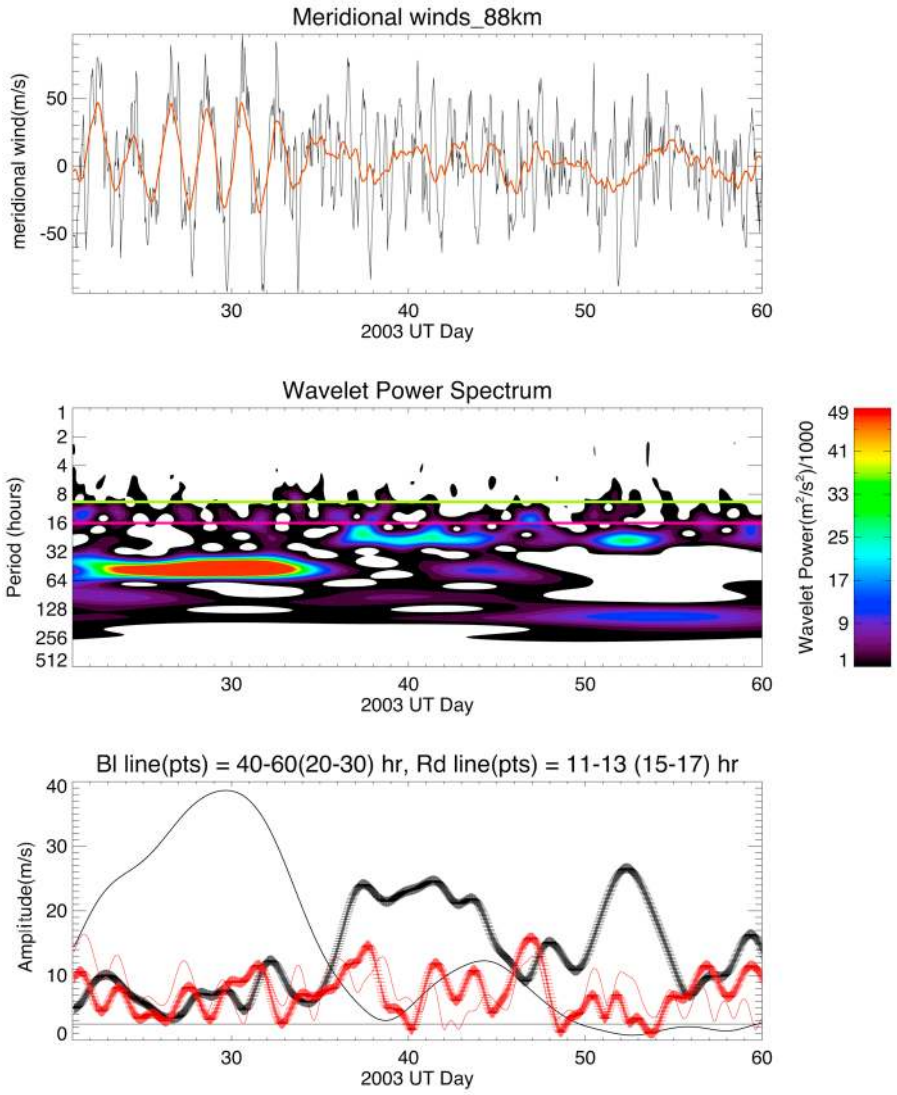

Figure 3. Same as Figure 2 but for the period from 0000 UT on 21 January 2003 to 0000 UT on 2 March 2003. The cone of influence is not shown.

weak near day 5 when the TDW is strong. However, from days 12 to 15 the diurnal tide strengthens as does the TDW. The semidiurnal tide is present for most of the period although there is some modulation of its amplitude. Horizontal lines are drawn at 16 and 9.6 h to guide the reader. From these it can be seen that both 16 and 9.6 h period waves appear to be strongest after day 12. Finally some longer multiday (4–6 day) period waves are present during the time when the TDW is strongest.

[26] Before discussing the strength of the main waves, it is important to understand the noise associated with this analysis. As noted before the wavelet analysis calculates the variance for four different band passes: 40–60 h for the TDW, 20–30 h for the diurnal tide, 15–17 h for the 16 h wave, and 11–13 h for the semidiurnal tide. In Figure 2 (bottom) those variances are converted into standard deviations which are equivalent to the wind amplitudes for that band pass. The horizontal line shows an estimate of the standard deviation in m/s expected in the 20–30 h band pass. This noise estimate is calculated from the MF radar variances at 88 km, discussed above, and Parseval's theorem to calculate how much of this variance would occur under each band pass assuming white noise [*Torrance and Compo*, 1998; *Hecht et al.*, 2007]. The noise estimates for the other band passes (not plotted) are between 1.5 and 2.5 m/s.

[27] Figure 2 (bottom) presents, more quantitatively, the strength of the main waves. In this first time interval up until day 17 the TDW wind amplitude slowly increases reaching a peak just below 30 m/s on day 15. The diurnal tide initially has a peak amplitude of 14 m/s but after day 363 of 2002 and until day 7 of 2003 the amplitude is on average about 7 m/s, sometimes dropping below 3 m/s. After day 7 the amplitudes for both the diurnal tide and the TDW increase together until day 15 after which they are anticorrelated. There also appears to be a 4–5 day modulation of the diurnal tide. The semidiurnal tide is present with amplitudes up to 12 m/s. It is modulated at times with a 2 day period. The 16 h wave only has an amplitude above the noise from day 9 to 15.

[28] Figure 3 shows results from 0000 UT on day 21 to 0000 UT on day 60. Figure 3 (top) shows a clear TDW

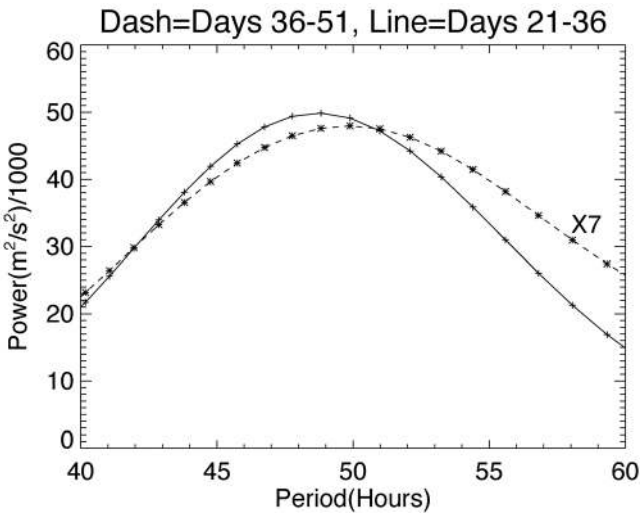

Figure 4. Plots of the summed wavelet power as function of Fourier period. The solid line is the sum over days 21 (21 January) to 36 (5 February) of 2003. The dashed line is the sum of days 36 (5 February) to 51 (20 February) of 2003 and multiplied by 7 for clarity.

signature that declines rapidly between days 33 and 35. Figure 3 (middle) shows that during most of this 12 day period the diurnal tide is absent or greatly suppressed. The semidiurnal tide, however, is present. During some of this time the 16 h wave is also apparent. The 9.6 h wave, however, is absent except around day 34 when the TDW is dissipating. After day 34 the diurnal tide is strong. Around day 42 it weakens. The TDW returns at day 40 and persists until day 48, after which it disappears. The strength of the 2 day wave is much less than in the period from day 21 to 34. A wave with a period near 4 days occurs during the time when the TDW is present. The 4 day wave disappears when the TDW disappears after day 50, being replaced with a wave whose period is above 6 days.

[29] Figure 3 (bottom) again presents wind amplitudes. From days 21 to 60, the TDW occurs in two bursts. In the first, over a 9 day interval, the amplitude (over a 40–60 h band pass) of the TDW increases to a peak of 37 m/s at day 30, and then in 6 days it dissipates to below 10 m/s. The amplitude of the diurnal tide (over a 20–30 h band pass) is almost perfectly anticorrelated with very low values, often below 7 m/s, until day 35. Then the diurnal tidal amplitude rapidly increases to 20 m/s. It declines rapidly on day 45 just at the point where the TDW amplitude has undergone a second minor amplification to almost 14 m/s. After a few more days the TDW amplitude has dissipated below the noise floor. The amplitude of the diurnal tide does the opposite; it increases.

[30] After the TDW disappears the amplitude of the diurnal tide wind component is about 20 m/s. During the peak period of the TDW the diurnal tidal wind has an amplitude of between 5 and 10 m/s. Thus, the diurnal tide wind amplitude is reduced by 50% to 75% when the strong TDW is present.

[31] During days 21–34 when the TDW amplitude is large, the amplitudes of the semidiurnal tide (over an 11–13 h band pass) and the 16 h wave (over a 15–17 h band pass) are well above the noise floor. They both appear to be modulated on a 2 day timescale mostly in phase with each other. Interestingly, the 16 h wave is strong near day 30, the peak day for the TDW, but somewhat out of phase with the occurrence of the semidiurnal tide.

[32] Figure 4 shows the power of the 40–60 h band as a function of Fourier period of the TDW during days 21–36 (second interval) and days 36–51 (third interval). A similar plot (not shown) was also produced for the first time interval ending at day 17. The peak of the power corresponds to the dominant Fourier period of the TDW. This varies from 46.8 to 48.9 to 50.1 h, respectively, for the three intervals. The first value is lower than what has been reported for the QTDW from the Northern Hemisphere but is consistent with some other Adelaide data for strong TDW events that have been attributed to the PL-TDW [*Harris*, 1994]. The second value is consistent with the 12 year average for the PL-TDW presented by *Harris* [1994]. The third value could be either a PL-TDW event based on *Harris* [1994] or simply a QTDW as found in the Northern Hemisphere or equatorial regions. It is interesting that the larger amplitude events occur at Fourier periods near and below 48 h while the smaller amplitude event has a larger Fourier period consistent with the QTDW. This will be addressed again later.

3.1.2. Airglow From Days 1 to 60, 2003

[33] Figures 5 and 6 show plots of the OHM and O2A intensity and temperature (designated as OHI, O2I, OHT, O2T in Table 1) from BP and AS. Also shown are the combined meridional wind data from Figures 2 and 3. The mean values of all airglow data taken in 2003 and 2004 and given in Table 1 are also shown as horizontal lines.

[34] Figures 5a, 5b, 6a, and 6b show the OHI and OHT results. At both BP and AS there is a large amplitude TDW oscillation from day 21 to approximately day 34 at BP and day 36 at AS. Table 1 also lists the frequency of occurrence for several arbitrary thresholds for airglow temperature and intensity. The peak values seen from days 30 to 34 are unusual events, and they are clearly due to the presence of a TDW. In fact, the highest OHI value of just over 5000 Rayleighs seen at BP is the also the highest seen to date (2002–2007) from any Australian OHI data.

[35] Next we focus on the second time interval (days 21–34) when the wind data show a peak in the PL-TDW around day 30. The airglow intensity time series data however, show a peak on day 33 after which, at BP, the 2 day modulation of the airglow abruptly ends. This is different than the wind response whose peak, from the wavelet analysis, occurs several days before the PL-TDW signature disappears. The airglow temperature peak is 2 days earlier than the airglow intensity peak. At AS the 2 day modulation continues for 2 days after it disappears at BP, ending on day 35. Finally, while the TDW response is, for the most part, clear in the OHI and OHT data it is less clear before day 30 in the O2I and O2T response. The phase relationship between the wind and airglow response can be seen from the vertical line on day 31 which is at the time of a minimum in the amplitude of the PL-TDW seen in the wind data. The airglow intensity and temperature are generally in phase, with an uncertainty of a few hours. With respect to the meridional wind component the airglow appears to be close to out of phase. In

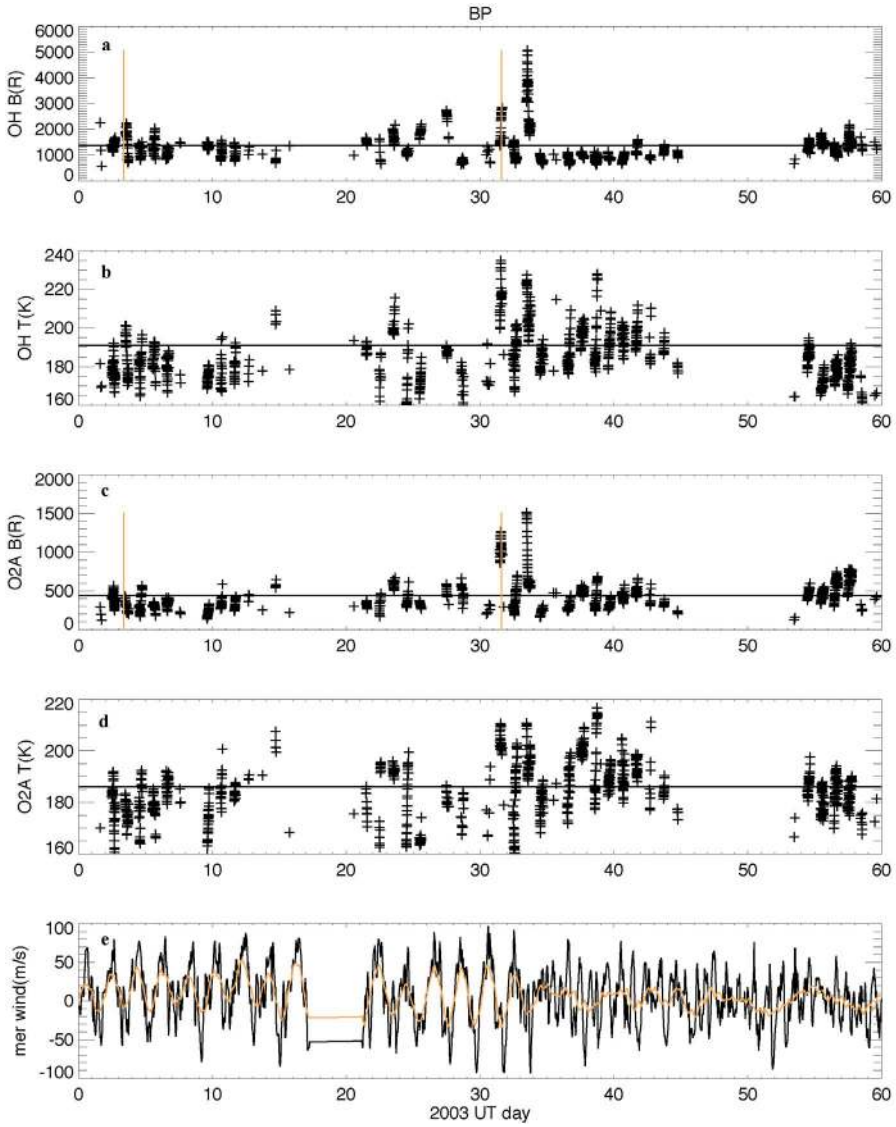

Figure 5. Data plots as a function of 2003 UT day. All data are from the site at Buckland Park (BP), Australia. (a) OH brightness in Rayleighs, (b) OH temperature, (c) O2A brightness in Rayleighs, and (d) O2A temperature. The horizontal lines show the mean values, from Table 1, for all the data (January to December) in 2003 and 2004. (e) Black line shows the meridional wind velocity in m/s. Orange line is a smooth of these data over 24 h. There is a data gap from days 17 to 21. The vertical lines in Figures 5a and 5c are two times where the 24 h smoothed wind data are at a minimum.

section 4 there will be a more quantitative discussion of some of these relationships.

[36] For the first time interval (up to day 17) the wind data showed a TDW variance that was a factor of two smaller than during the second interval. From days 1 to 7 the diurnal tide is suppressed and the dominant variation in the wind is due to a TDW. The airglow response is also smaller during this period but a clear TDW signature can be seen in the OHI and OHT data from BP and in the OHT data from AS. In the O2I and O2T data from BP a signature also appears to be present. However, while the OHT data maintain an out of phase relationship with the wind data for this period the O2T data appear to be in phase. At AS no clear TDW modulation is seen in the O2 data.

3.2. Data From 2004–2006

[37] Figures 7–9 present, for the years 2004–2006, a subset of results as was just discussed for 2003. In this section comments will be restricted to pointing out differences or notable similarities. The results for the summed periods of 20–30 and 40–60 h are shown in Figure 8 (top) while those for 11–13 and 15–17 h are shown in Figure 8 (bottom).

3.2.1. Meridional Winds

[38] Figures 7 and 8 show abbreviated results for the meridional wind analysis for 2004, 2005, and 2006. The data from 2005 resembles that of 2003 in both the timing of the major peak and its amplitude. The data from 2004 and 2006 are similar to each other, with the date of the peak occurring earlier and being of lower amplitude than in 2003 and 2005.

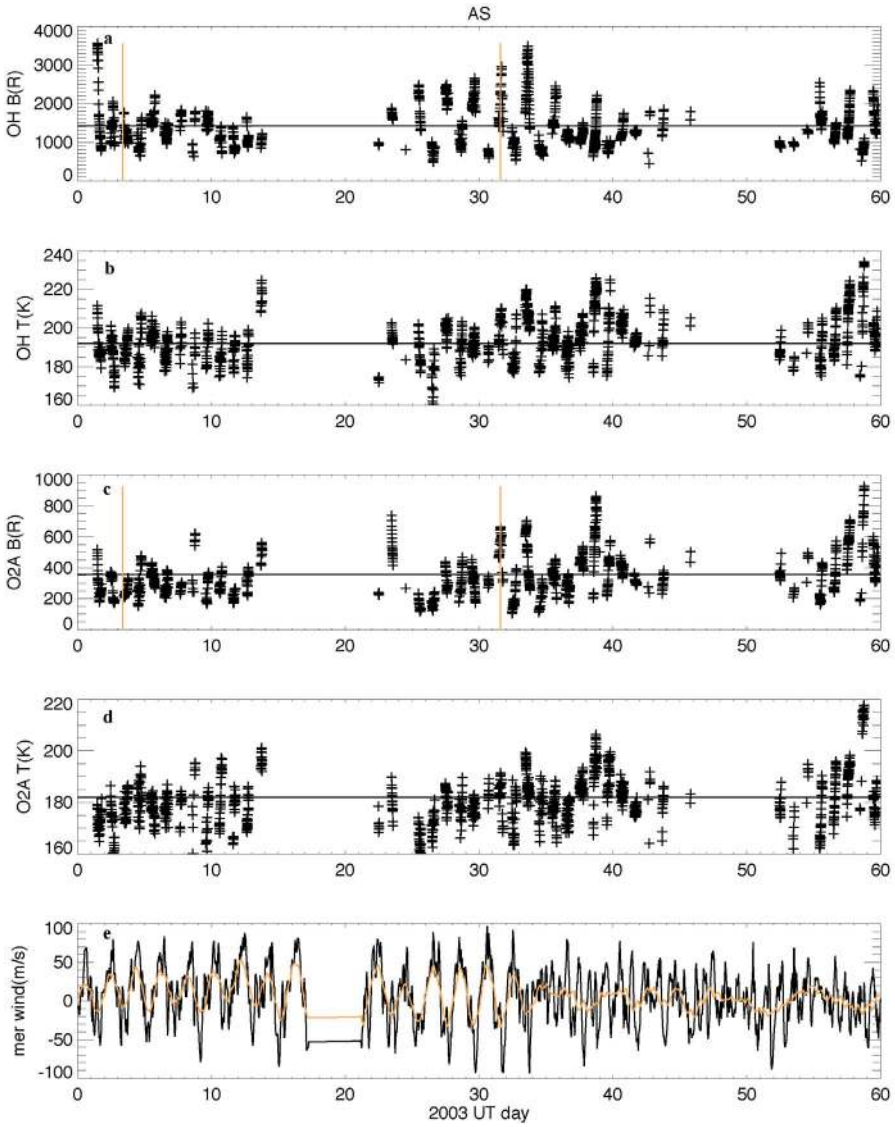

Figure 6. (a–d) Same as Figure 5 except the data are from Alice Springs (AS), Australia. (e) The wind data are the same as in Figure 5 and are from Buckland Park.

3.2.1.1. Data From 2004

[39] In 2004 while the amplified TDW may last almost as long as was found in 2003 its peak amplitude was only about half as great. Unlike 2003 the TDW had rapid amplification near day 7 but had a gradual decline from the peak which lasted on the order of 20 days. The mean Fourier period of the TDW is not shown but was found to be 46 h. Thus, a PL-TDW was probably present during some or all of this period. The diurnal tide amplitude was not as suppressed as in 2003. Here during the time interval of the amplified TDW the diurnal tide wind speed was, much of the time, about 40 to 50% of that seen after the TDW dissipated. Interestingly, there were three periods when the diurnal tide was greatly suppressed, at day 2, day 10, and day 15. These were all periods when the TDW underwent amplification. These also occurred as the TDW was increasing in amplitude. During the declining TDW phase, after day 15, the diurnal tide did not show any change when the TDW suddenly increased. However, the general anticorrelation between the TDW and the diurnal tide was present; that is the diurnal tide amplitude was much smaller when the TDW amplitude was large and vice versa. With respect to the other waves of interest there did not seem to be a strong 2 day modulation of the amplitude of semidiurnal tide, and the 9.6 h wave was not noticeably strong. The 16 h wave is above the noise floor for almost the entire period from day 12 to day 28 during which the TDW is strong.

3.2.1.2. Data From 2005

[40] In 2005 the largest amplitude TDW (which is slightly off scale at a peak amplitude just below 45 m/s) occurs between days 21 and 35 similar to 2003; during this period the diurnal tide is greatly suppressed with some periods during which there is no detectable diurnal tide. However, the transition period between large-amplitude TDW and small-amplitude diurnal tide to small-amplitude TDW and large-amplitude diurnal tide is not as sharp as the 1 day

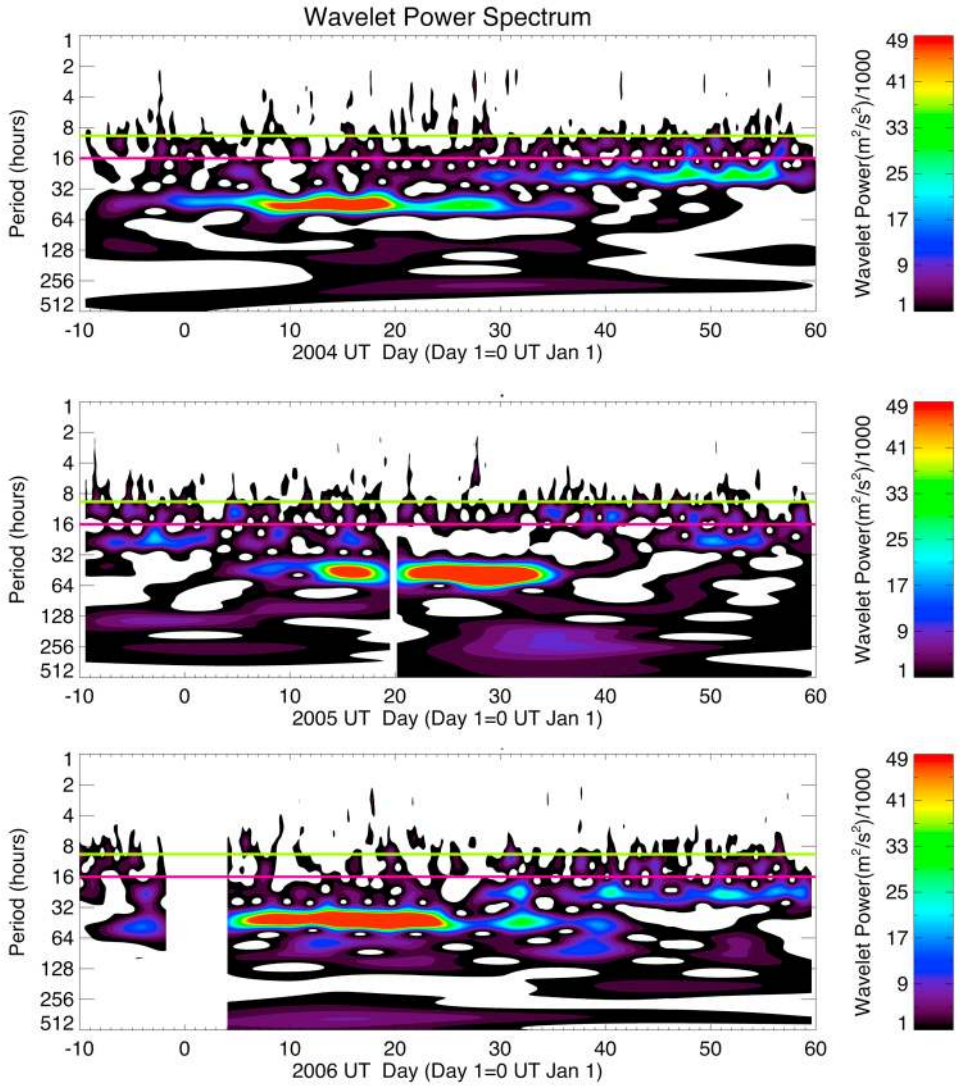

Figure 7. Same as Figures 2 (middle) and 3 (middle). The *x* axis runs from (top) 0000 UT on 21 December 2003 to 0000 UT on 29 February 2004, (middle) 0000 UT on 21 December 2004 to 0000 UT on 1 March 2005, and (bottom) 0000 UT on 21 December 2005 to 0000 UT on 1 March 2006. Data were missing in the vertical white areas in 2005 and 2006. The wavelet analysis was done separately in the two data periods of 2005 and in 2006.

transition found in 2003. The peak amplitude of near 44 m/s is the largest of the 4 years reported on here. Interestingly, during days 25–30 when the diurnal tidal amplitude is close to the noise floor, the 16 h amplitude is greatest. While the semidiurnal tide is also somewhat depressed during this time interval there is little evidence of a 9.6 h wave. As was found during 2003 there is a near 2 day modulation of the semidiurnal tidal amplitude. The mean period of the TDW, determined from an analysis similar to that shown in Figure 4, is just below 50 h similar to 2003.

3.2.1.3. Data From 2006

[41] In 2006 the TDW is present until day 43 although it is largest between days 10 and 25 similar to what was observed in 2004. Also, as was found in 2004, the diurnal tide is only partly suppressed with an amplitude decrease of only about 50%. The peak TDW amplitude of around 32 m/s is above the observed values in 2004 but below that observed in 2003 and 2005. For the most part there does not appear to be a 2 day modulation of the semidiurnal tide. Around day 20 when the TDW amplitude peaks, there is a decrease in the diurnal tidal amplitude and an increase in the 16 h wave amplitude. There is also a peak in the 9.6 h wave amplitude. The mean Fourier period of the TDW is 42.5 h, a value well below 48 h as was found in 2004.

3.2.2. Airglow

3.2.2.1. Data From 2004

[42] Figure 9 shows some airglow results for BP and AS. At BP there are only data for five nights during the main TDW period through about day 20. These nights do include the night of the peak TDW amplitude at day 15. The OHI

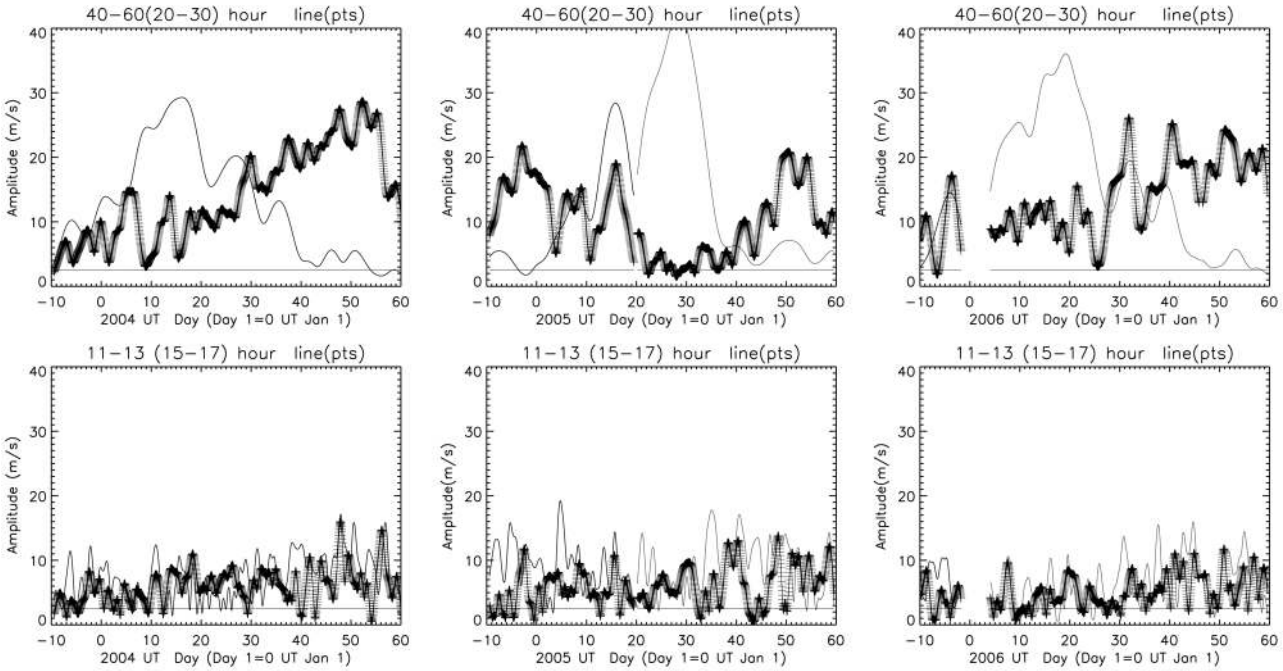

Figure 8. (top) Same as Figure 2 (bottom) but only showing 20–30 and 40–60 h band passes for the time period from (left) 0000 UT on 21 December 2003 to 0000 UT on 29 February 2004, (middle) 0000 UT on 21 December 2004 to 0000 UT on 1 March 2005, and (right) 0000 UT on 21 December 2005 to 0000 UT on 1 March 2006. (bottom) Same as Figure 8 (top) but for sums over 11–13 and 15–17 h.

airglow response shows a maximum near 2500 R, well above the long-term average. There is also a clear 2 day modulation of the OHI. For O2I (not shown) there is little measurable response to the presence of a TDW.

[43] At AS there are considerable more data with nightly measurements from day 10 to day 28. As at BP there is a clear 2 day wave modulation of the OHI. The greatest response occurs between days 10 and 20 consistent with the wind amplitude. The other airglow plots (OHT, O2I, O2T) show a much less obvious response, perhaps due to the presence of other stronger waves with larger periods than the TDW.

3.2.2.2. Data From 2005–2006

[44] There are less airglow data in 2005 and 2006 than in previous years for several reasons. With respect to the period when the TDW amplitude was large, moon up and overcast conditions were more extensive during these years than in 2003/2004. Also in 2006 there was no airglow imager located at BP, only at AS. The 2006 data at AS suffered from moon up conditions between days 10 and 20 so as to make any analysis of marginal validity.

[45] In 2005, though, there are some useful data. At BP there is enhanced OHI (above 3000 R) on day 21 as well as a clear 2 day modulation between days 10 and 20. However, while there are enhanced intensities, above 2000 R, on days 21, 23, and 25 the intensities from days 29 to 31 do not appear unusually high. The O2I intensities are high (above 600 R) on days 18 and 21, and also show a 2 day modulation before day 20. But because so much data are missing in the period between days 20 and 35 it is difficult to say much more. At AS there is somewhat better coverage, although there are data gaps between days 20 and 30. While there is some 2 day modulation in all of the data sets there does not appear to be the same large enhancements around days 34 and 35 as was seen in the 2003 data set.

4. Discussion

4.1. Relationship of the PL-TDW and the Diurnal Tide

[46] Given the data presented above we can now address how the diurnal tide varies due to the presence of a TDW which may be characterized as a PL-TDW. However, before that discussion we address to what extent the TDW was actually phase-locked during the periods that were analyzed (i.e., had a Fourier period close to 48 h).

[47] While in 2003 the mean Fourier period is close to (but slightly above) 48 h, during the other years the deviation from 48 h is greater. To investigate this Figure 10 shows a time history of the Fourier period of the TDW which is obtained by contouring the amplitudes of the wind wavelet power between 40 and 60 h that were plotted in Figures 2, 3, and 7. Figure 10 suggests that the two pairs of odd-numbered years and even-numbered years each have similar characteristics. For example, in the even-numbered years the largest peaks in TDW amplitude occur at times when the Fourier period is below 48 h, varying between 43 and 46 h. In the odd-numbered years the largest peaks occur at or above 48 h.

[48] A more detailed discussion with respect to the diurnal tide will first be applied to the even-numbered years where the peak TDW amplitude and the suppression of the diurnal tide are both lower than was found in the odd-numbered

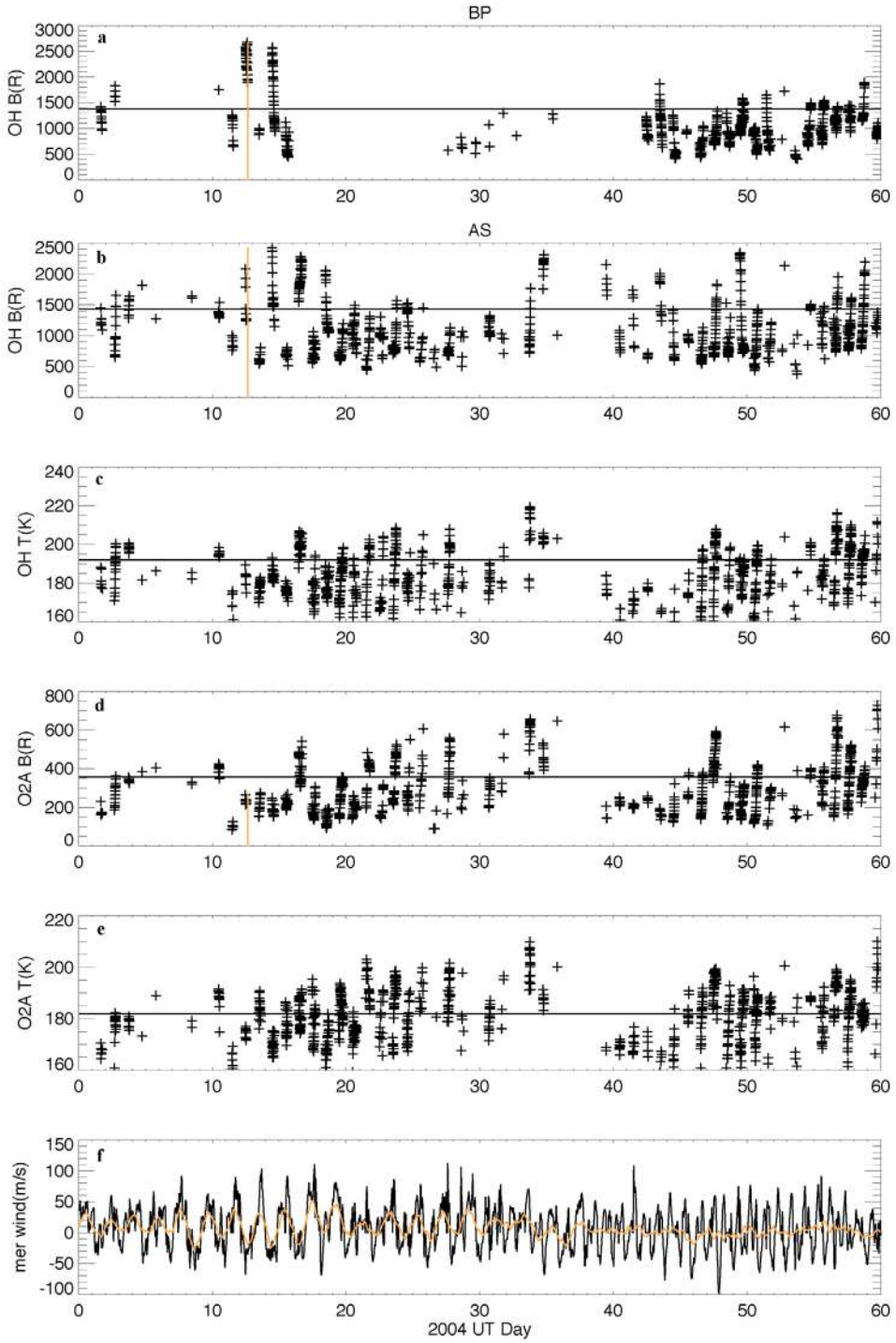

Figure 9. Similar to Figure 5 except that all data are from 2004. (a) OHI data from BP. (b) OHI, (c) OHT, (d) O2I, and (e) O2T are data from Alice Springs (AS). (f) Meridional wind data from BP.

years. In 2004 just before day 10 the Fourier period is about 48 h and there is a rapid amplification of the TDW. The diurnal tide also decreases. However after day 10 when the Fourier period is near 46 h, there is not much additional increase in the TDW amplitude and the diurnal tidal amplitude stays well above the noise floor. In 2006 the wave Fourier period is always below 46 h, there is no period of rapid amplification, and the diurnal tide is also above the noise. Nevertheless, even in these cases the decrease in the diurnal tidal amplitude is about twice that predicted by the TIMED-GCM analysis of *Palo et al.* [1998].

[49] In both 2003 and 2005 there were data gaps between days 17 and 21 so the analysis in Figure 10 is broken into two time intervals. For both years for the first interval the

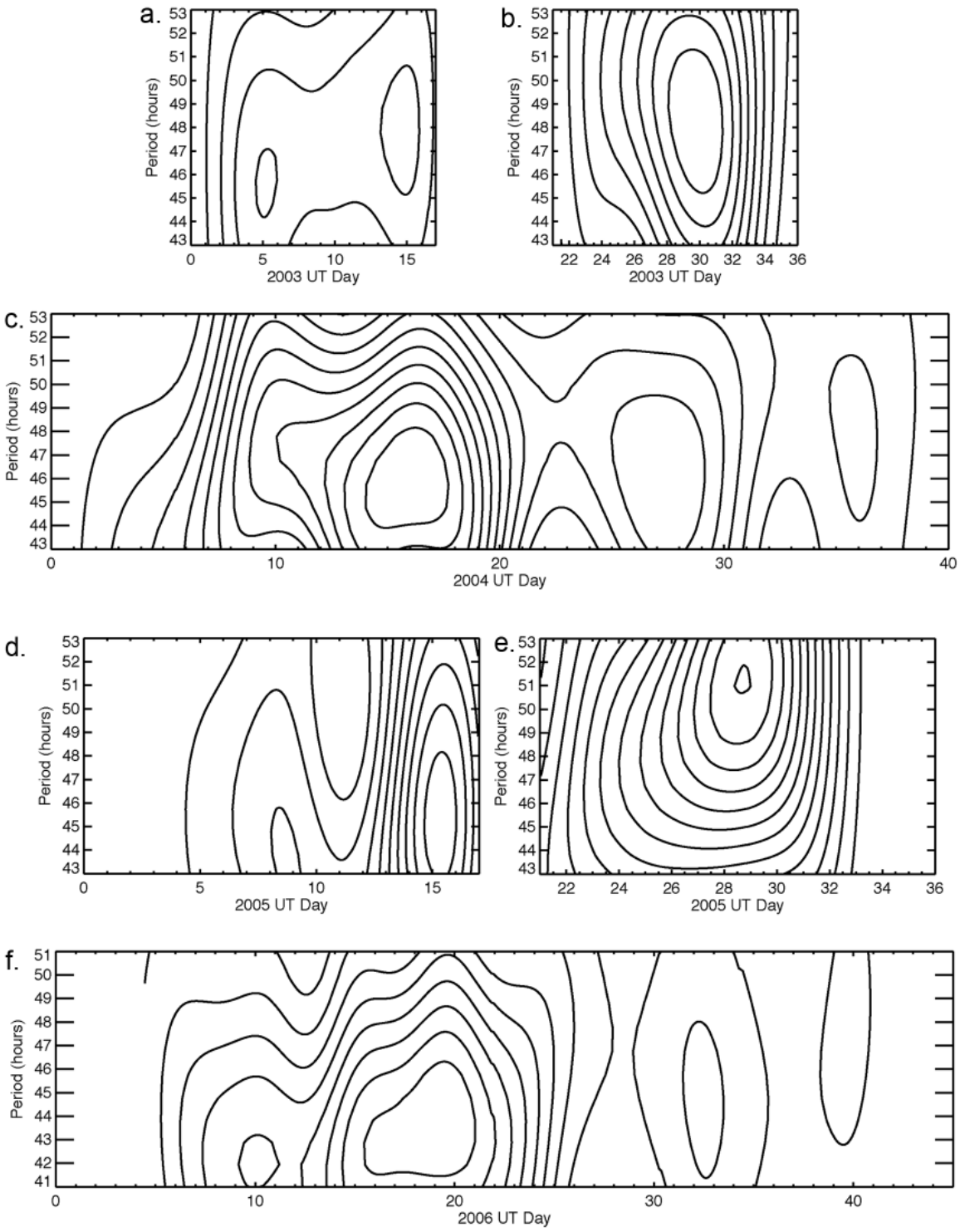

Figure 10. Contours of the wavelet power for the years 2003–2006 as function of Fourier period. The wavelet power is the same as is found in the Figures 2 (middle), 3 (middle), and 7 (middle). The value for the first contour (the spacings) are as follows: (a) 8000 (2003 days 0–17), (b) 7270 (2003 days 21–36), (c) 3130 (2004), (d) 2730 (2005 days 0–17), (e) 6240 (2005 days 21–36), and (f) 7270 (2006). The lowest-valued contour is on the left for all plots except Figure 10b, where it occurs on the right.

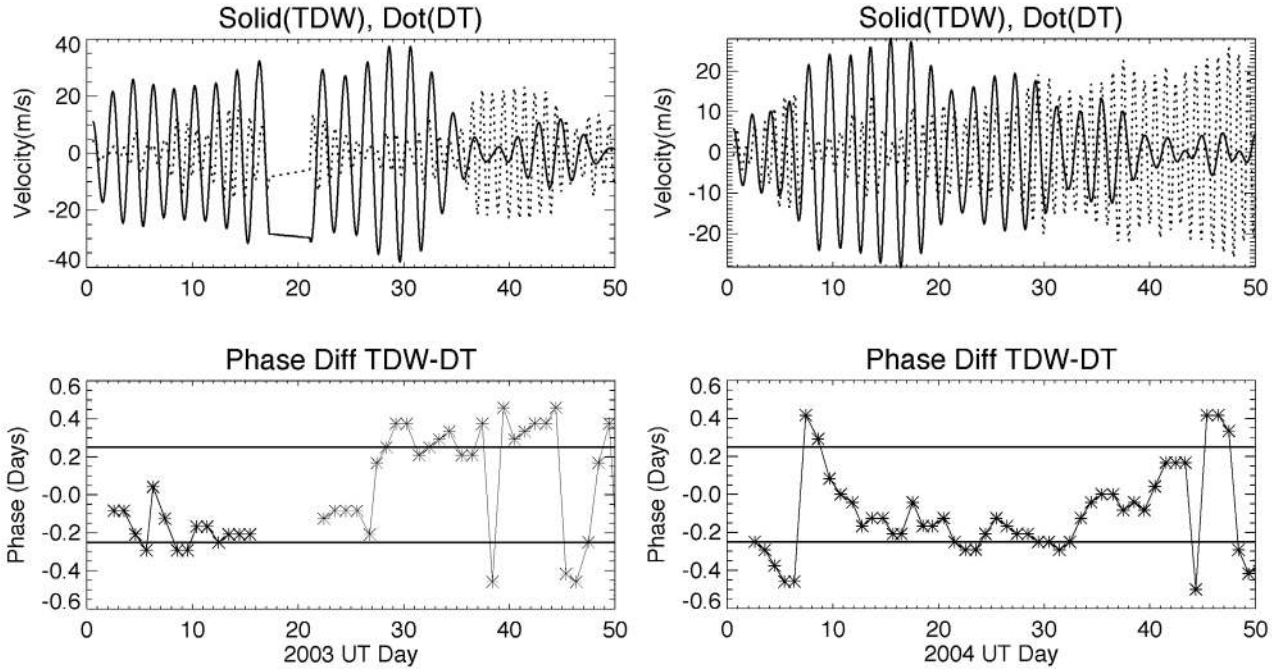

Figure 11. Data are for (left) 2003 and (right) 2004. (top) Wavelet reconstruction of the wind velocities in the 40–60 h TDW (solid line) and 20–30 h diurnal tide (dotted line) band pass. (bottom) Phase difference in days between the maxima and minima of the TDW and the maxima of the diurnal tide velocities. In Figure 11 (bottom) the horizontal lines are at ±0.25 days.

TDW amplitudes are lower than in the second time interval. For the first time interval the Fourier periods are for the most part below 48 h. Interestingly, as was found in 2004, the period of rapid amplification near day 13 of 2005 corresponded to an interval when the wave Fourier period briefly changed from above 48 h to below 48 h.

[50] During the second time interval, after day 21, in both 2003 and 2005 the TDW reached a maximum and the diurnal tide was almost completely suppressed. In 2003 the TDW Fourier period is very close to 48 h at the peak. In 2005, before day 26 the wave Fourier period is close to 48 h. However, after that the TDW Fourier period increases to almost 52 h a value that was observed at days 28–30 the time of the maximum. After day 30 there is a rapid decrease in the TDW although the diurnal tide does significantly increase until day 40. In both 2003 and 2005 the suppression of the diurnal tide, during the period when the TDW amplitude is large, is much greater than during the even-numbered years or that predicted by *Palo et al.* [1998].

[51] The suppression of the diurnal tide in all 4 years occurs during the period when the TDW is large. Furthermore, these data show the amplification of the TDW is greatest when its Fourier period is close to 48 h, and thus a PL-TDW. This is consistent with the model of *Walterscheid and Vincent* [1996] which suggests that the amplification is due to a parametric excitation of the TDW by the diurnal tide. Although the day in 2005 when the largest observed TDW amplitude occurred was when the Fourier period was above 48 h, we note that just prior to that day the TDW Fourier period was 48 h and the excitation could have occurred at that time.

[52] To further investigate the suppression of the diurnal tide during TDW events the phase between them was investigated. The wavelet technique allows a direct reconstruction of the wave signal in the 40–60 h and 20–30 h band passes which are in fact nearly identical to the amplitudes shown in Figures 2, 3, and 8. The former are calculated directly from the real part of the wavelet while the latter are the square root of the wavelet power and these different techniques produce different roundoff errors. Figure 11 shows these reconstructions for the first 50 days of years 2003 and 2004 during which the TDW maximized and then diminished. Using these data the difference in the phase of the maxima or minima of the TDW and the closest maximum of the diurnal tide was calculated. These are also shown in Figure 11. There will be some uncertainty in this result since during some periods in 2003 (and in 2005) the diurnal tide is greatly suppressed and during such times finding a maximum is difficult. What seems to be remarkable is that for the most part there seem to be two different states. During some of the time of the TDW the phase difference is slightly negative (with the TDW leading the tide) and at other times the two waves are close to out of phase. This again seems consistent with the idea of a PL-TDW. *Walterscheid and Vincent* [1996] noted that repeatability of the phase of the TDW relative to the tide strengthens the connection inferred from observations between the tides and the TDW, though the precise phase relations is not predicted by the theory. However, there are still some interesting questions. associated with this phase relationship. Why for example, does the PL-TDW still exist after day 30 of 2003 (with a period close to 48 h) if the phase locking has changed?

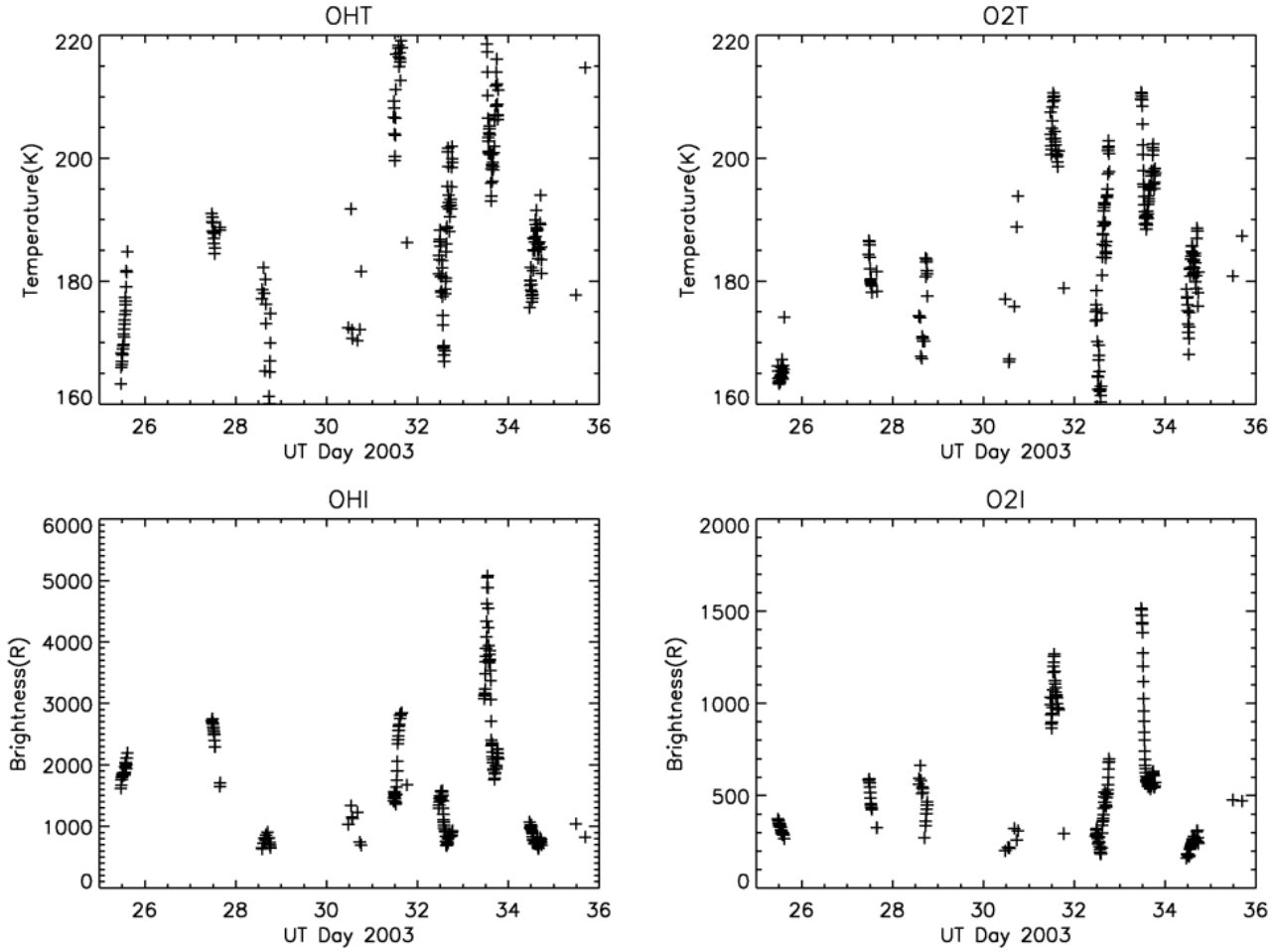

Figure 12. OHM and O2A intensities (OHI and O2I) and temperatures (OHT and O2T) at BP for days 25–36 of 2003.

Similarly, why does the phase locking to the diurnal tide of the PL-TDW in 2004 also take a few days?

[53] The data described above also show several periods when the TDW amplified, the diurnal tide became more suppressed, and there was an increase in the 16 h wave. This phenomenon is also consistent with an exchange of energy between the diurnal tide and the TDW since such an interaction would produce a 16 h wave.

4.2. Relationship of the PL-TDW and the Semidiurnal Tide

[54] In 2003 and 2005 there is a noticeable 2 day modulation of the semidiurnal tide with little evidence of the 9.6 h wave. Thus, there does not appear to be much of an exchange of energy between the semidiurnal tide and the PL-TDW with respect to the amplification of the PL-TDW. Rather, in some way the PL-TDW is modulating the semidiurnal tide, perhaps by changing the background state seen by the tide.

[55] In 2004 and 2006 the 2 day modulation is less evident and there are some periods when the 9.6 h wave is present. Thus, in those years there may be some exchange of energy between these two waves.

4.3. Phase Relation of the PL-TDW Wind Field to the Temperature

[56] The airglow data provide the temperature response to the presence of the PL-TDW. Unfortunately, the airglow data are not continuous over 48 h, typically being measured over about 10 h each night, so the exact phase relationship between the winds and temperatures is somewhat uncertain.

[57] In order to better quantify this phase relationship we examined the airglow temperature response at BP from days 25 to 36 in 2003 (as shown in Figure 12), a time when the diurnal tide was suppressed and the PL-TDW response in the wind data was strong. At BP around day 30 of 2003 we found that the time of the PL-TDW wind maximum/minimum was around 1430 UT or approximately 2400 LT. An examination of the airglow data indicate that a maximum or minimum also occurred between 1200 and 1700 UT. The maximum in the airglow data occurred when the wind data showed a minimum and vice versa. The airglow intensity and temperature peaks appear to be less than 2 h out of phase as discussed below. These data suggest that the meridional wind and the temperature are close to out of phase. There is an uncertainty in this conclusion, since even though the diurnal tide was suppressed there were other

waves present that could complicate the interpretation. These include the semidiurnal tide and the 16 h wave, both of which appear in the wavelet analysis of the wind data, and an 8 h period wave which is discussed in section 4.4.

[58] Nevertheless, it is interesting that airglow observations show, at least for these days, phase maxima and minima close to local midnight, a time when airglow observations can be measured from the ground. If the maxima in the PL-TDW meridional wind were at 0430 UT (1400 LT), as was found in the earlier work of *Harris* [1994], and assuming, as we found, that the wind and temperature are out of phase the nighttime airglow response would be minimal since the phase of the PL-TDW would be near a node.

[59] We note though that the PL-TDW, if indeed resonant is a Lamb wave, and idealized Lamb waves have a quadrature phase relationship between the temperature and the meridional wind (see Appendix A). Physically, the pressure and meridional component must be in quadrature for idealized steady state normal mode oscillations on a sphere. This is because these modes are standing waves in the meridional direction and therefore the meridional energy flux ($\overline{\nu' p'}$) must vanish, and by equation (A3) given in Appendix A the quantity ($\overline{\nu' T'}$) = 0, where the overbar denotes a zonal average [*Longuet-Higgins*, 1968]. The fact that our observations indicate that T' and ν' are closer to being in antiphase than in quadrature indicates that the wave is not a steady state global mode, but is forced regionally and is exporting energy from the region where the wave is forced. The observed antiphase relation between T' and ν' indicates that $\overline{\nu' T'} < 0$, or an equatorward flux of heat if the observed phase relation holds around a circle of latitude. To the extent that peaks in airglow fluctuations represent maxima or minima in the minor constituents involved in airglow chemistry, the observed airglow phases indicate a meridional minor constituent flux.

4.4. Airglow Response to the PL-TDW

[60] The fortuitous timing of the maxima/minima near local midnight allows a characterization of the response of the airglow temperature and intensity to the PL-TDW. The analysis uses the OHI and OHT data, as shown in Figures 12 and 13, from both BP and AS during days 25–36 in 2003.

[61] Because continuous daily data are required to investigate the airglow PL-TDW response we concentrate on data from days 27 to 28 and 30 to 35 at BP. Day 29 data are missing. Examination of the OHI data at BP suggest that peak values occur in the interval from 1200 to 1700 UT. However, there are other waves present, such as the semidiurnal tide, and any phase relationship between OHI and OHT is uncertain. The data are averaged over 6 h centered on 1424 UT each day. This averaging time period was chosen because (1) data are available during this period, (2) this minimizes the influence of other waves on the estimation of the airglow PL-TDW amplitude, and (3) has a minimal effect on the amplitude of the airglow PL-TDW. Nevertheless there is some uncertainty in the exact phase of the PL-TDW and this is discussed further below. Tables 2–5 summarize the results of the analysis.

[62] First we will discuss the OHM results at BP with an emphasis on perturbations inferred from the temperature data from days of 30 to 36. The second and third columns of Table 2 show the temperature and intensity averages. There are clear oscillations on a 2 day timescale seen in these data. The fourth column shows the fractional change in temperature ($\Delta T/T$) calculated by taking the absolute value of the change between the given day and the previous day divided by the average value for those 2 days. (Since as can be seen in Figure 12 there were missing days, there are gaps in the rows of days 27 and 30.) The largest value occurs on day 31 and there is a day to day decrease for every subsequent day. Following *Walterscheid and Schubert* [1990] the fifth column shows estimates of the equivalent wind amplitude computed using (g/N)($\Delta T/T$), where g is the acceleration due to gravity and N is the Brunt-Vaisala frequency. Here, N is calculated isothermally using the mean temperature. These estimates can be compared to the sixth column, the measured amplitude of the PL-TDW wind perturbation. After day 30 the wind speeds inferred from this approximation are in reasonable agreement. Note though, that on day 28 the winds are a factor of two smaller. It is unclear if other long-period waves were present before day 30 at BP (see Figure 3) that may be modifying the temperature response.

[63] The fact that the winds inferred from the temperature perturbations are close to the measured winds has another implication. That is the temperature and wind are close to out of phase rather than being in quadrature. If the latter were occurring, and given the fact that the wind maxima occur near midnight (during the middle of the airglow observation period) one would expect that the airglow perturbations would be small since the phase of the airglow PL-TDW would be near a node.

[64] The intensity perturbations ($\Delta I/I$) are shown in the seventh column. These show a distinctly different trend, increasing from day 31 to day 34 with the largest value occurring on day 34, after which there is a sharp falloff.

[65] The last column shows the ratio of the intensity to temperature perturbations a quantity known as η, the Krassovsky ratio [e.g., *Schubert et al.*, 1991]. *Walterscheid and Schubert* [1995] have calculated, for OHM, η values for Rossby planetary waves and found amplitudes near 2 with a phase shift near 15° between the intensity and temperature response. While on days 31 and 35 the η values are near 2, on the days with the largest intensity perturbations (days 33 and 34) the values are much higher. These results, and also that for day 28, suggest that there are other effects, besides a pure wave response, that are amplifying the airglow intensity perturbations. One possibility may be the constituent transport discussed in sections 1 and 4.3.

[66] Some additional evidence for processes that modify the airglow intensity at BP is found in the O2A results shown in Table 3. Until day 34 the trend in $\Delta T/T$ is similar to what was found in OHM. However for $\Delta I/I$ the peak occurs on day 31 and except for day 34 decreases throughout the period. The η values are similar to those found for OHM on days 31 to 33 but higher on days 34 to 36. Thus, for both OHM and O2A there is a much greater response in intensity than in temperature.

[67] Tables 4 and 5 show the results for AS. These data (as seen in Figure 13) show a clear 2 day oscillation in both intensity, and, for the most part, in temperature from day 25 to day 36. Since wind data are not available from AS these results can be used to infer a wind perturbation. The inferred

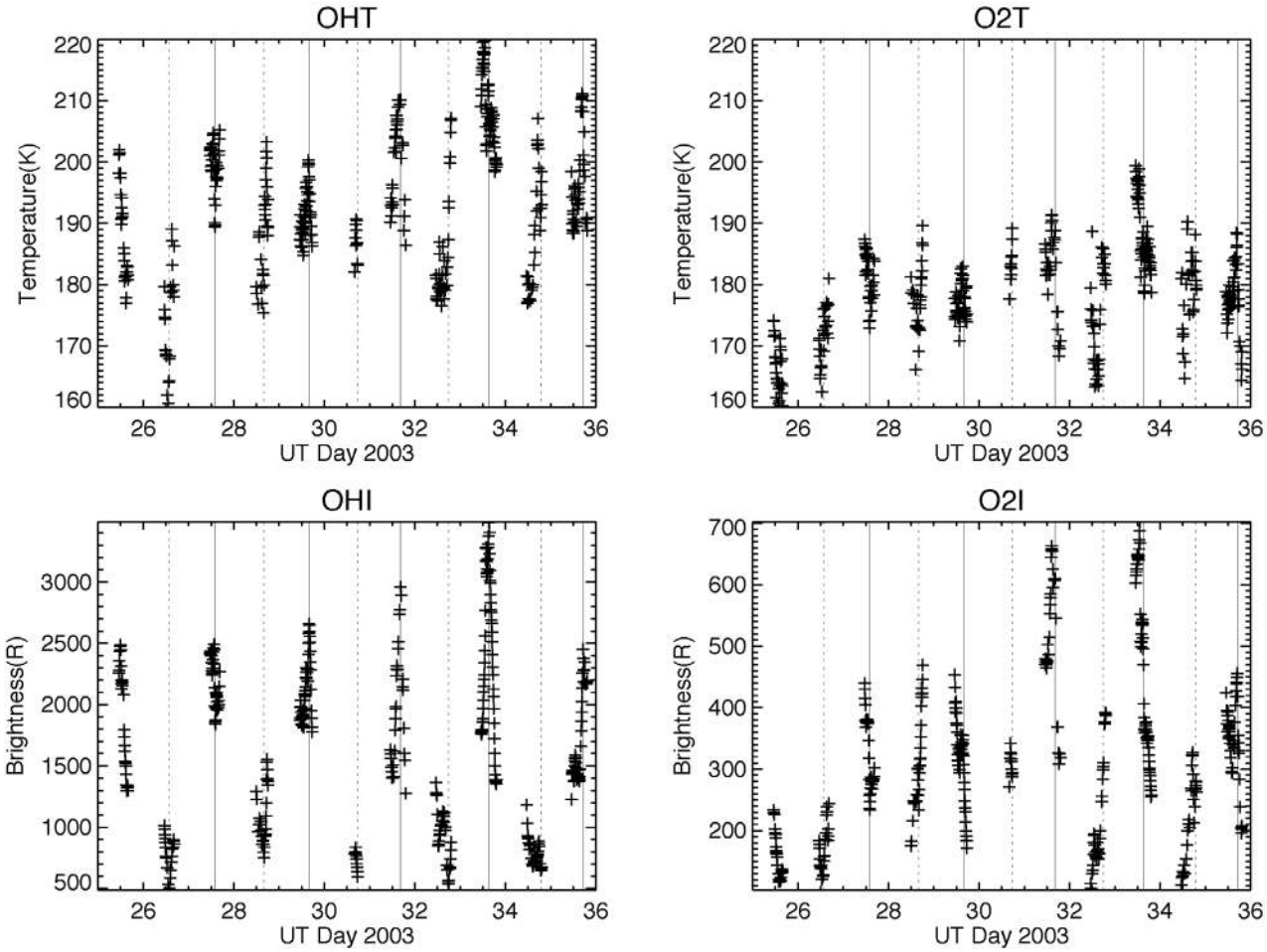

Figure 13. OHM and O2A intensity (OHI and O2I) and temperature (OHT and O2T) at AS for days 25–36 of 2003. The vertical lines represent the times of a maximum (solid line) or minimum (dotted line) in the OHI data, which would be associated with a maximum or minimum in the 2 day wave response of the airglow.

wind perturbations are lower than at BP except on days 33 and 34 when they are somewhat higher. Unlike BP the largest airglow temperature response occurs during the days when the airglow intensity response is also the largest. The η values are quite high again suggestive of additional processes modifying the composition.

[68] On the days when the BP wind and temperature responses were largest (days 30–31) the AS temperature responses are the smallest. This could be due to a weaker PL-TDW on those days at AS. However, the net result is that for OHM the η values on those days are much larger at AS than at BP. The same is true for O2A. These anomalous results on days 30–31 could be due to composition changes, or some variation in the phase relationship between the temperature and meridional wind.

[69] Figure 13 also gives some information on the phase differences between the airglow data. Vertical lines show the time of a maximum or minimum of the OHI airglow.

Table 2. BP OHM Airglow

Day	T (K)	B (R)	$\Delta T/T$ (%)	$(g/N)\Delta T/T$ (m/s)	V (m/s)	$\Delta I/I$ (%)	η
27	188.1	2438.0		0	34		
28	173.8	768.0	3.9	16	36	52.0	13.2
30	175.5	1175.2			37		
31	216.2	2051.6	10.3	46	35	27.1	2.6
32	183.1	1100.5	8.3	37	31	30.1	3.6
33	208.1	3331.7	6.3	28	26	50.3	7.9
34	184.2	809.7	6.1	27	19	60.8	10.0
35	196.2	932.5	3.2	13	12	7.0	2.2
36	183.3	885.1	3.4	14	7	2.6	0.8

Table 3. BP O2A Airglow

Day	T (K)	B (R)	$\Delta T/T$ (%)	$(g/N)\Delta T/T$ (m/s)	V (m/s)	$\Delta I/I$ (%)	η
27	181.7	478.0			34		
28	171.1	531.6	3.0	12	36	5.3	1.8
30	167.9	235.3			37		
31	204.2	1049.8	9.7	42	35	63.3	6.5
32	176.5	327.3	7.2	31	31	52.4	7.2
33	196.0	821.2	5.2	22	26	43.	8.2
34	180.0	226.3	4.2	18	19	56.7	13.3
35	184.1	473.6	1.1	4	12	35.3	31.1
36	183.9	282.3	0.0005	0	7	25.3	555.7

Table 4. AS OHM Airglow

Day	T (K)	B (R)	ΔT/T (%)	(g/N)ΔT/T (m/s)	V (m/s)	ΔI/I (%)	η
25	188.3	1894.1			28		
26	174.2	754.2	3.8	16	31	43.0	11.1
27	199.4	2212.1	6.7	29	34	49.1	7.3
28	184.1	957.9	3.9	17	36	39.5	9.9
29	191.7	2147.1	2.0	8	37	38.2	18.9
30	186.5	801.8	1.3	6	37	45.6	32.7
31	201.5	1994.8	3.8	17	35	42.6	11.0
32	180.5	1045.5	5.5	24	31	31.2	5.7
33	211.1	2653.5	7.8	34	26	43.4	5.6
34	182.3	835.9	7.3	32	19	52.0	7.1
35	196.0	1525.7	3.6	15	12	29.2	8.1
36	188.8	1193.8	1.8	8	7	12.2	6.5

As can be seen within a few hours the OHI and OHT (for days 31–33) data are in phase. This would be consistent with the models for the response of airglow to Rossby waves discussed previously. However, other wavelike oscillations (gravity waves or tidal modes) may be distorting this somewhat so the exact phase relationship with respect to hours is somewhat uncertain.

[70] Figure 14 shows a more detailed look at the OHM intensity variations for periods covering from one to three full PL-TDW cycles. Figure 14 (top) shows data for days 31, 32, and 33 at BP. On days 31 and 33 there appears to be a strong wavelike variation during the night. However, on day 32 this wave is suppressed.

[71] Figure 14 (middle) shows the same 3 days but for observations obtained at AS where the nightly data coverage was somewhat more extensive. On days 31 and 33 there are similar large wavelike features during the night. To investigate this three additional plots are shown, each of which has as one component a wave with a period of 48 h and a phase maximum at 1224 UT, 2 h earlier than what was inferred above. The solid line shows such a wave with an amplitude of 850 R. The dashed line on the right shows this wave combined with an additional 8 h wave whose amplitude is 900 R and which peaks at 1628 UT. These parameters were chosen to provide a visual best fit to the data. The dashed line on the left shows a visual best fit to the feature on day 31. Here the 48 h wave is of slightly lower amplitude (750 R) and the 8 h wave is also of slightly different amplitude and phase. We note that while the width of the feature is narrow enough to preclude it being due to a 12 h tide it could be due to a 9.6 h wave, especially if the features shape is being perturbed by other waves. Nevertheless an 8 h wave provided a better visual fit and appears to be the cause of the feature.

[72] An 8 h period wave can result either through a combination of the 24 and 12 h tides or through a combination of a 9.6 h wave and a 48 h wave such as the PL-TDW. The 9.6 h wave can form, as noted earlier, from an interaction of the 12 h tide and the PL-TDW. Thus, in either path the 8 h wave (or indeed a 9.6 h wave) depends on a strong 12 h tide. The meridional wind analysis also showed that the PL-TDW modulated the strength of the semidiurnal tide with a large amplitude on days 31 and 33 and a low amplitude on day 32. Thus, one might expect the 8 h wave to follow the same pattern and it does. Why the 8 h waveforms so strongly on these two nights however is not clear.

[73] Figure 14 (bottom) addresses the possible difference in the phase maximum of the TDW between BP and AS. While Figure 14 (top) suggested that at BP the phase maximum in the PL-TDW occurred at 1224 UT, Figure 14 (bottom) plots a 48 h wave for 6 days of OHI data using 1424 UT as a phase maximum. Given the limited data it appears there is an uncertainty as to when the maximum occurs. That can only be resolved by obtaining a longer data set.

[74] The data for both sites also suggest that, with respect to intensity, the OHM airglow is showing the TDW response more consistently than the O2A airglow. For example, as seen in Figure 13 around day 30 in 2003 the OHM airglow is showing a strong 2 day oscillation not seen in the O2A airglow. One possibility for this is that the TDW is being damped first at higher altitudes where the O2A emission is occurring and later at the 88 km altitude used for this study where the OHM emission layer peaks. To address this Figure 15 plots the amplitudes for the TDW and the diurnal tide at 88, 92, and 94 km. As can be seen the TDW is only slightly lower in amplitude at 92 and 94 km than at 88 km during the period of the PL-TDW prior to day 35. Thus, it does not appear that damping is the reason for the different response in the O2A and OHM layers. Figure 15 does illustrate one intriguing result though. The diurnal tide seems to recover earlier at 92 and 88 km than at 94 km after the TDW amplitude has greatly decreased starting around day 35.

[75] Finally, it should be noted that outside the core period of the strongest PL-TDW, around days 25–35 in 2003 and days 10–20 in 2004, the TDW signal in airglow is small. During the core periods the airglow response in intensity is much above the mean airglow intensity levels as shown in Table 1. While a 2 day oscillation signal may be present in some of the airglow data (e.g., prior to day 7 in 2003 and after day 20 in 2004) outside these core periods, the airglow amplitudes are small and, as noted above, perhaps masked by other wave signals. During these noncore periods the mean airglow levels are consistent with the yearly means. Why this is so is not apparent at this time. However, we also note that the TDW is a Lamb wave (as are all free modes) and prototypical Lamb waves have zero vertical velocity. This means that, unlike for gravity waves and tides, vertical transport would play no role in driving an airglow response. Lamb waves in realistic atmospheres do not necessarily have zero vertical velocity (especially during periods of

Table 5. AS O2A Airglow

Day	T (K)	B (R)	ΔT/T (%)	(g/N)ΔT/T (m/s)	V (m/s)	ΔI/I (%)	η
25	166.6	155.5			28		
26	171.6	172.6	1.4	6	31	4.9	3.3
27	181.0	327.0	2.6	11	34	30.8	11.6
28	174.8	258.2	1.7	7	36	11.6	6.7
29	177.2	334.6	0.6	2	37	12.7	19.0
30	179.8	314.4	0.7	3	37	3.1	4.2
31	185.3	555.4	1.5	6	35	27.7	18.3
32	170.4	156.9	4.1	17	31	55.9	13.4
33	189.2	533.8	5.2	22	26	54.5	10.5
34	177.7	170.2	3.1	13	19	51.6	16.5
35	179.3	367.8	0.4	1	12	36.7	79.6
36	174.9	293.5	1.2	5	7	11.2	8.9

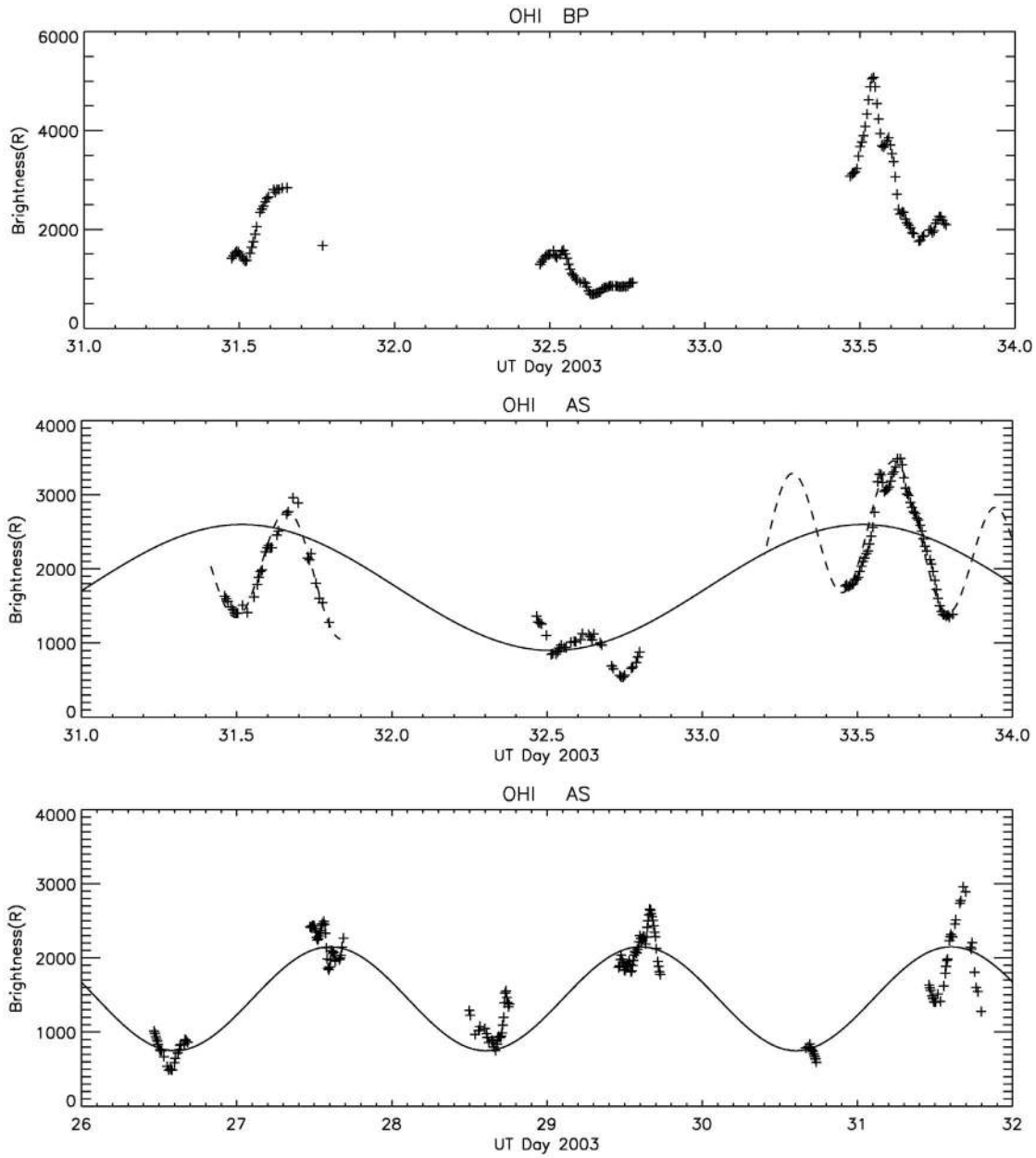

Figure 14. (top) OHI at BP for days 31–34 of 2003. (middle) Same as Figure 14 (top) but for AS. The solid line is a wave of 48 h period with an amplitude of 850 R and whose peak is at 1224 UT. The dashed line at right combines this with an 8 h period wave of 900 R amplitude and a peak at 1618 UT. The dashed line at left combines the 48 h wave of amplitude 650 R and a peak at 1618 UT with an 8 h wave of 750 R amplitude and a peak at 1557 UT. (bottom) OHI at AS for days 26–32. The solid line is a 48 h wave that peaks at 1424 UT with an amplitude of 700 R.

transient change), but there may be times when the airglow response is subdued because vertical transport is essentially nil.

5. Conclusions

[76] In this study we have analyzed wind and airglow data, at two sites in Australia for the approximate 2 month period after austral summer solstice. During this time period a large amplitude TDW has always been observed with a mean Fourier period close to 48 h and thus is a PL-TDW. The data sets from 2003 to 2006 that are analyzed in this paper were used to address three questions.

[77] 1. What is the relationship of the diurnal and the semidiurnal tide to the PL-TDW? During periods of a large amplitude PL-TDW the amplitude of the diurnal tide was suppressed by as much as 75%. This was larger than predicted by TIME-GCM model runs previously reported on

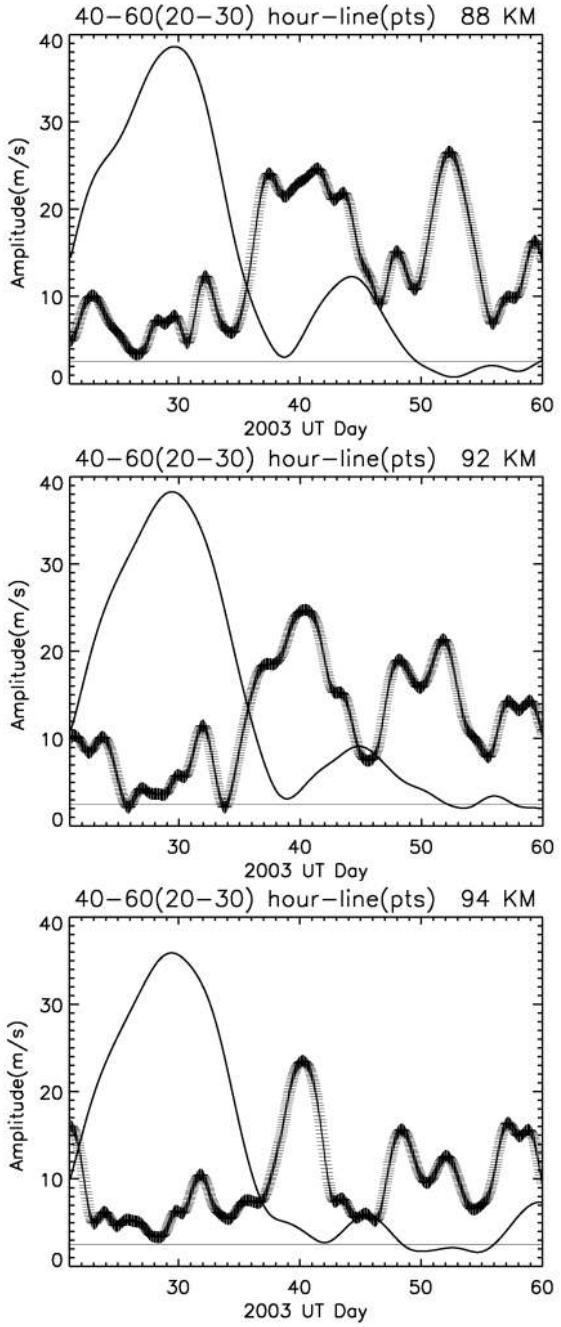

Figure 15. Meridional wind amplitude (in m/s) for wavelet periods of 40–60 h (black solid line) and 20–30 h (black pluses). (top) 88 km altitude, (middle) 92 km altitude, and (bottom) 94 km altitude.

by *Palo et al.* [1998]. The large anticorrelation between them is consistent with the model of *Walterscheid and Vincent* [1996] in which the amplification of the PL-TDW (when its period is close to 48 h) is due to a parametric excitation by the diurnal tide.

[78] The data also showed that the suppression of the diurnal tide was larger in 2003 and 2005 than in 2004 and 2006. This maybe related to the period of the TDW, since we found that there were also interannual differences in that quantity. In 2003 the mean Fourier period was close to 48 h and in 2005 the Fourier period went from below to above 48 h at the time when the TDW amplitude was either amplifying or at its largest. In 2004 and 2006 the TDW Fourier period was almost always below 48 h. These results suggest that what we refer to as the PL-TDW refers to those TDWs whose mean period is at or somewhat below 48 h, a condition that appears to occur frequently in the austral summer while the QTDW has a period that is at or above 50 h a condition that occurs nearly all of the time in the Northern Hemisphere. The coupling of the diurnal tide appears to be more efficient when the PL-TDW period is close to 48 h resulting in a larger diurnal tidal amplitude as observed. When the period stays well below 48 h the coupling of the diurnal tide to the PL-TDW appears less efficient. Whether the observed biannual variation for these 4 years of the suppression of the diurnal tide is related to other processes such as the QBO needs further investigation. Specifically, future work is needed to establish the persistence of this biannual effect.

[79] The semidiurnal tide was found to vary in amplitude with a 2 day period. In 2003 and 2005 there was little evidence of a direct energy exchange between this tide and the PL-TDW. In 2004 and 2006 however, the 9.6 h wave was present at times suggesting some exchange of energy between the semidiurnal tide and the PL-TDW.

[80] 2. What is the variation of temperature during PL-TDW events? The temperature variations were generally consistent, with respect to amplitude, with what would be expected from the wind variations. However, at AS on days 29–30 when the BP wind data suggested an amplitude maximum in the PL-TDW the temperature variations were small. One explanation for this was a decrease in the PL-TDW at AS during those days.

[81] The temperature was found to vary close to out of phase with the wind, with both showing maxima/minima around midnight local time. Given this out-of-phase relationship, the time of the peak temperature is different than what would be expected from the meridional wind data previously reported by *Harris* [1994] who found a peak in the wind data around 1400 LT.

[82] The temperature wind phase relation is not consistent with what would be expected if the PL-TDW was an idealized Lamb wave. These results imply that the PL-TDW wave is not a steady state global mode, but is forced regionally and is exporting energy from the region where the wave is forced.

[83] 3. What is the airglow response during a PL-TDW event?

[84] The airglow intensity response was in general much larger than what would be expected from the airglow temperature response. This suggests that the PL-TDW is causing a significant composition change possibly due to minor constituent transport. This is consistent with the wind-temperature phase relation noted above. Thus, to the extent that peaks in airglow fluctuations represent maxima or minima in the minor constituents involved in airglow chemistry, the observed airglow phases indicate a meridional minor constituent flux.

[85] There appears in some of the 2003 OHI data to be a large 8 h period wave that occurs with a 2 day modulation of its amplitude. This indirectly implies a 2 day modulation of

the semidiurnal tide an effect that was also seen in the meridional wind data.

Appendix A

[86] In this appendix we show that there is a quadrature relation for idealized Lamb waves (Lamb waves on a resting basic state). Lamb waves are characterized by a vertical velocity perturbation, w', that is identically zero. The first law is

$$c_p \frac{dT}{dt} = \frac{1}{\rho} \frac{dp}{dt} \tag{A1}$$

where T is the temperature, t is time, ρ is density, p is pressure, and c_p is the specific heat at constant pressure. With a windless basic state and $w' \equiv 0$ the linearized version of (A1) is

$$c_p \frac{\partial T}{\partial t} = \frac{1}{\rho} \frac{\partial p}{\partial t} \tag{A2}$$

whence

$$\frac{T'}{\overline{T}} = \kappa \frac{p'}{\overline{p}} \tag{A3}$$

where the overbar represents a background quantity, and κ is R/c_p where R is the gas constant. Since v', the meridional velocity perturbation, is in quadrature with $p'/\overline{p}$ quadrature is demonstrated between the meridional wind and temperature [see *Chapman and Lindzen*, 1970, chapter 18, equation 3].

[87] **Acknowledgments.** Thanks to Peter Strickland and Jeremy Ward for the considerable help at Alice Springs. The Aerospace Corporation's results could not have been obtained without the invaluable help given by Kirk Crawford in all aspects of this project. J.H.H., R.L.W., and L.J.G. were supported by NSF grants ATM-0737557 and ATM-0436516 and by NASA grant NNX08AM13G. R.A.V. acknowledges support from Australian Research Council grant DP0558361. The initial version of the wavelet software was provided by C. Torrance and G. Compo and is available at http://paos.colorado.edu/research/wavelets/.

References

Chapman, S., and R. S. Lindzen (1970), *Atmospheric Tides*, 201 pp., Gordon and Breach, New York.

Craig, R. L., and W. G. Elford (1981), Observations of the quasi 2-day wave near 90 km altitude at Adelaide (35°S), *J. Atmos. Terr. Phys.*, *43*, 1051–1056.

Doyle, E. M. (1968), Wind measurements in the upper atmosphere, Ph.D. thesis, Univ. of Adelaide, Adelaide, South Aust., Australia.

Fritts, D. C., J. R. Isler, R. S. Lieberman, M. D. Burrage, D. R. Marsh, T. Nakamura, T. Tsuda, R. A. Vincent, and I. M. Reid (1999), Two-day wave structure and mean flow interactions observed by radar and High Resolution Doppler Imager, *J. Geophys. Res.*, *104*, 3953–3969, doi:10.1029/1998JD200024.

Gelinas, L. J., J. H. Hecht, R. L. Walterscheid, R. G. Roble, and J. M. Woithe (2008), A seasonal study of mesospheric temperatures and emission intensities at Adelaide and Alice Springs, *J. Geophys. Res.*, *113*, A01304, doi:10.1029/2007JA012587.

Hagan, M., J. Forbes, and F. Vial (1993), Numerical investigation of the propagation of the quasi-two-day wave into the lower thermosphere, *J. Geophys. Res.*, *98*, 23,193–23,205, doi:10.1029/93JD02779.

Harris, T. J. (1994), A long-term study of the quasi-two-day wave in the middle atmosphere, *J. Atmos. Terr. Phys.*, *56*, 569–579.

Harris, T. J., and R. A. Vincent (1993), The quasi-two-day wave observed in the equatorial middle atmosphere, *J. Geophys. Res.*, *98*, 10,481–10,490, doi:10.1029/93JD00380.

Hecht, J. H. (2004), Instability layers and airglow imaging, *Rev. Geophys.*, *42*, RG1001, doi:10.1029/2003RG000131.

Hecht, J. H., R. L. Walterscheid, and M. N. Ross (1994), First measurements of the two-dimensional horizontal wavenumber spectrum from CCD images of the nightglow, *J. Geophys. Res.*, *99*, 11,449–11,460, doi:10.1029/94JA00584.

Hecht, J. H., R. L. Walterscheid, D. C. Fritts, J. R. Isler, D. C. Senft, C. S. Gardner, and S. J. Franke (1997), Wave breaking signatures in OH airglow and sodium densities and temperatures: 1. Airglow imaging, Na lidar, and MF radar observations, *J. Geophys. Res.*, *102*, 6655–6668, doi:10.1029/96JD02619.

Hecht, J. H., R. L. Walterscheid, M. P. Hickey, and S. J. Franke (2001), Climatology and modeling of quasi-monochromatic atmospheric gravity waves observed over Urbana Illinois, *J. Geophys. Res.*, *106*, 5181–5196, doi:10.1029/2000JD900722.

Hecht, J. H., A. Z. Liu, R. L. Walterscheid, R. G. Roble, M. F. Larsen, and J. H. Clemmons (2004a), Airglow emissions and oxygen mixing ratios from the photometer experiment on the Turbulent Oxygen Mixing Experiment (TOMEX), *J. Geophys. Res.*, *109*, D02S05, doi:10.1029/2002JD003035.

Hecht, J. H., S. Kovalam, P. T. May, G. Mills, R. A. Vincent, R. L. Walterscheid, and J. Woithe (2004b), Airglow imager observations of atmospheric gravity waves at Alice Springs and Adelaide, Australia during the Darwin Area Wave Experiment (DAWEX), *J. Geophys. Res.*, *109*, D20S05, doi:10.1029/2004JD004697.

Hecht, J. H., A. Z. Liu, R. L. Walterscheid, S. J. Franke, R. J. Rudy, M. J. Taylor, and P.-D. Pautet (2007), Characteristics of short-period wavelike features near 87 km altitude from airglow and lidar observations over Maui, *J. Geophys. Res.*, *112*, D16101, doi:10.1029/2006JD008148.

Hickey, M. P., G. Schubert, and R. L. Walterscheid (1993), Gravity wave-driven fluctuations in the O_2 atmospheric (0-1) nightglow from an extended, dissipative emission region, *J. Geophys. Res.*, *98*, 13,717–13,729, doi:10.1029/92JA02348.

Holdsworth, D. A., and I. M. Reid (2004), The Buckland Park MF radar: Routine observation scheme and velocity comparisons, *Ann. Geophys.*, *22*, 3815–3828.

Lima, L. M., P. P. Batista, H. Takahashi, and B. R. Clemesha (2004), Quasi-two-day wave observed by meteor radar at 22.7°S, *J. Atmos. Sol. Terr. Phys.*, *66*, 529–537.

Longuet-Higgins, M. S. (1968), The eigenfunctions of Laplace's tidal equations over a sphere, *Phil. Trans. R. Soc. London A*, *262*, 511–607.

Manson, A. H., and C. E. Meek (1990), Long period (~8–20 h) wind oscillations in the upper middle atmosphere at Saskatoon (52°N): Evidence for non-linear tidal effects, *Planet. Space Sci.*, *38*, 1431–1441.

Muller, H. G., and L. Nelson (1978), A travelling quasi 2-day wave in the meteor region, *J. Atmos. Terr. Phys.*, *40*, 761–766.

Palo, S. E., R. G. Roble, and M. E. Hagan (1998), TIME-GCM results for the quasi-two-day wave, *Geophys. Res. Lett.*, *25*, 3783–3786, doi:10.1029/1998GL900032.

Pancheva, D. V. (2006), Quasi-2-day wave and tidal variability observed over Ascension Island during January/February 2003, *J. Atmos. Sol. Terr. Phys.*, *68*, 390–407.

Pancheva, D. V., et al. (2006), Two-day wave coupling of the low-latitude atmosphere-ionosphere system, *J. Geophys. Res.*, *111*, A07313, doi:10.1029/2005JA011562.

Plumb, R. A. (1983), Baroclinic instability of the summer mesosphere: A mechanism for the quasi-two-day wave?, *J. Atmos. Sci.*, *40*, 262–270.

Plumb, R. A., R. A. Vincent, and R. L. Craig (1987), The quasi-two-day wave event of January 1984 and its impact on the mean mesospheric circulation, *J. Atmos. Sci.*, *44*, 3030–3036.

Rodgers, C. D., and A. J. Prata (1981), Evidence for a traveling two-day wave in the middle atmosphere, *J. Geophys. Res.*, *86*, 9661–9664.

Salby, M. L. (1981), The 2-day wave in the middle atmosphere: Observations and theory, *J. Geophys. Res.*, *86*, 9654–9660.

Schubert, G., R. L. Walterscheid, and M. P. Hickey (1991), Gravity wave-driven fluctuations in OH nightglow from an extended, dissipative emission region, *J. Geophys. Res.*, *96*, 13,869–13,880.

Takahashi, H., L. M. Lima, C. M. Wrasse, M. A. Abdu, I. S. Batista, D. Gobbi, R. A. Buriti, and P. P. Batista (2005), Evidence on 2–4 day oscillations of the equatorial ionosphere h'F and mesospheric airglow emissions, *Geophys. Res. Lett.*, *32*, L12102, doi:10.1029/2004GL022318.

Torrance, C. T., and G. P. Compo (1998), A practical guide to wavelet analysis, *Bull. Am. Meteorol. Soc.*, *71*, 61–78.

Tsuda, T., S. Kato, and R. A. Vincent (1988), Long period wind oscillations observed by the Kyoto meteor radar and comparison of the quasi-2-day

wave with Adelaide HF radar observations, *J. Atmos. Terr. Phys.*, *50*, 225–230.

Walterscheid, R. L., and G. Schubert (1990), Nonlinear evolution of an upward propagating gravity wave: Overturning, convection, transience and turbulence, *J. Atmos. Sci.*, *47*, 101–125.

Walterscheid, R. L., and G. Schubert (1995), Dynamical-chemical model of fluctuations in the OH airglow driven by migrating tides, stationary tides, and planetary waves, *J. Geophys. Res.*, *100*, 17,443–17,449.

Walterscheid, R. L., and R. A. Vincent (1996), Tidal generation of the phase-locked 2-day wave in the Southern Hemisphere summer by wave-wave interactions, *J. Geophys. Res.*, *101*, 26,567–26,576.

Ward, W. E., B. H. Solheim, and G. G. Shepherd (1997), Two day wave induced variations in the oxygen green line volume emission rate: WINDII observations, *Geophys. Res. Lett.*, *24*, 1127–1130.

L. J. Gelinas, J. H. Hecht, and R. L. Walterscheid, Space Sciences Department, The Aerospace Corporation, PO Box 92957, Mail Stop M2-260, Los Angeles, CA 90009, USA. (lynette.gelinas@aero.org; james.hecht@aero.org; richard.walterscheid@aero.org)

I. M. Reid, R. A. Vincent, and J. M. Woithe, Department of Physics and Mathematical Physics, University of Adelaide, Adelaide, SA 5005, Australia. (iain.reid@physics.adelaide.edu.au; robert.vincent@physics.adelaide.edu.au; jwoithe@physics.adelaide.edu.au)